INVESTIGATING THE EFFECTIVENESS OF WHEAT STARCH AND POLYMERIC ADDITIVES ON THE PRODUCTION OF BIOMEDICAL THERMOPLASTIC STARCH COMPOSITES

BİYOMEDİKAL TERMOPLASTİK NİŞASTA KOMPOZİTLERİNİN ÜRETİMİNDE BUĞDAY NİŞASTASI VE POLİMERİK KATKILARIN ETKİNLİĞİNİN İNCELENMESİ

NAZLI KHAGHANIMILANI

PROF. DR. MENEMŞE GÜMÜŞDERELİOĞLU

Supervisor

Submitted to

Graduate School of Science and Engineering of Hacettepe University

as a Partial Fulfillment to the Requirements

for the Award of the Degree of Master of Science

in Bioengineering.

2023

ABSTRACT

INVESTIGATING THE EFFECTIVENESS OF WHEAT STARCH AND POLYMERIC ADDITIVES ON THE PRODUCTION OF BIOMEDICAL THERMOPLASTIC STARCH COMPOSITES

Nazli KHAGHANIMILANI

Master of Science, Department of Bioengineering
Supervisor: Prof. Dr. Menemşe Gümüşderelioğlu
February 2023, 74 pages

The presence of natural polymers as biomaterials has had a desirable efficacy on the development and progress of medical science research. Starch is a natural polymer that is abundant in nature, cost-effective, biodegradable, biocompatible, and non-toxic that has been recognized as a biomaterial with the potential to use in tissue engineering and pharmaceutical various fields of experiments.

Practically, numerous hydrogen bonds amongst starch macromolecules make starch decompose, before reaching the melting point, under rising temperature conditions. This property can limit the usage of starch in different situations of research, however by modifying starch to thermoplastic starch (TPS), the mentioned problem can almost be solved. Conversion of starch to TPSs, improve the raw starch's physical, chemical, mechanical, and functional abilities, which is the first aim of the research, where the next goal of the study is to evaluate the effects of different type and the ratio of plasticizers in fabricated TPS films' mechanical and chemical properties to be able to choose the right options for use in tissue engineering research. Starch granules in the presence of water, heat, and shear condition by mixing with plasticizers like glycerol and D-sorbitol, which are

approved by the Food and Drug Administration (FDA), undergo disruption, which causes a homogeneous melt named TPS. The last aim of the current research is to investigate TPS films' biocompatibility and cytotoxicity properties by seeding normal human dermal fibroblast (n-HDF) cells on them.

In this study, Thermoplastic wheat starch (TPS) films were fabricated with 30% to 70% total plasticizer with different ratios of glycerol and D-sorbitol by solution casting method. Wheat starch due to its higher amylose content which can increase tensile strengths and young's modulus of the TPS was selected in fabricating the TPS films. The plasticizers portion of the films was altered from 30% to 70% depending on the starch weight (3 g). After the mechanical test, from this point of view, six TPS films were selected for the advanced analysis due to their pioneer mechanical properties.

Generally, TPS Films with total plasticizers of 30% and 40% presented higher tensile strength, toughness, and elastic modulus values in comparison to films with a total plasticizer of 50%, 60%, and 70%. Increment in the ratio of the D-sorbitol to glycerol in TPS films with equal total plasticizers had led to higher density value and thermal stability, however, reduces moisture absorption, and hydrolytic degradation ratio of the TPS films. Three groups of the films with 60% (20S-40G), 50% (20S-30G), and 40% (10S-30G) plasticizers, presented higher biocompatibility and proper surfaces for cells adhesion and proliferation, from the normal human dermal fibroblast cells viability analysis. Overall, TPS films showed better mechanical and physical properties at lower percentages of plasticizer, on the contrary, in cell studies, an increment in the percentages of plasticizers led to higher cell adhesion and viability, therefore increasing the biocompatibility of the TPS films.

Keywords: Starch, D-Sorbitol, Glycerol, Thermoplastic starch, Normal human dermal fibroblast cells, Tissue engineering

ÖZET

BİYOMEDİKAL TERMOPLASTİK NİŞASTA KOMPOZİTLERİNİN ÜRETİMİNDE BUĞDAY NİŞASTASI VE POLİMERİK KATKILARIN ETKİNLİĞİNİN İNCELENMESİ

Nazli KHAGHANIMILANI

Yüksek Lisans, Biyomühendislik Anabilim Dalı

Tez Danışmanı: Prof. Dr. Menemşe Gümüşderelioğlu

Şubat 2023, 74 Sayfa

Biyomalzeme olarak, doğal polimerlerin varlığı, biyomedikal bilim araştırmalarının gelişimi ve ilerlemesi üzerinde önemli bir etkinliğe sahiptir. Nişasta, doğada bol bulunan, uygun maliyetli, biyobozunur, biyouyumlu ve toksik olmayan doğal bir polimerdir ve doku mühendisliği ve farmasötik çeşitli deney alanlarında kullanım potansiyeli olan bir biyomateryal olarak kabul edilmiştir. Pratik olarak, nişasta makromolekülleri arasındaki sayısız hidrojen bağları, nişastanın artan sıcaklık koşulları altında erime noktasına ulaşmadan ayrışmasına neden olur. Bu özellik, farklı araştırma durumlarında nişasta kullanımını sınırlayabilir, ancak nişastanın termoplastik nişastaya (TPN) dönüştürülmesiyle bahsedilen sorun neredeyse çözülebilir. Araştırmanın ilk amacı olan nişastanın TPN'ye dönüştürülmesi, ham nişastanın fiziksel, kimyasal, mekanik ve fonksiyonel yeteneklerinin

geliştirilmesi dir ve çalışmanın bir sonraki amacı, doku mühendisliği araştırmalarında kullanım için doğru seçenekleri seçebilmek için üretilen TPN filmlerin mekanik ve kimyasal özelliklerinde farklı tip ve oranlarda plastikleştiricilerin etkilerini değerlendirmektir. Gıda ve İlaç Dairesi (FDA) onaylı gliserol ve D-sorbitol gibi plastikleştiriciler ile karıştırılarak su, ısı ve kesme koşulunda, nişasta granülleri bozulmaya uğrar ve bu da TPS olarak adlandırılan homojen bir eriyik oluşmasına neden olur. Mevcut araştırmanın son amacı, TPS filmlerinin üzerine normal insan dermal fibroblast (n-HDF) hücrelerini ekerek biyouyumluluk ve sitotoksisite özelliklerini araştırmaktır. Bu çalışmada, termoplastik buğday nişastası (TPN) filmleri, çözelti döküm yöntemi ile farklı oranlarda gliserol ve D-sorbitol ile %30 ile %70 toplam plastikleştirici ile üretilmiştir. TPS'nin gerilme mukavemetlerini ve Young modülü artırabilen yüksek amiloz içeriği nedeniyle buğday nişastası TPN filmlerini üretmek için seçildi. Filmlerin plastikleştirici oranları nişasta ağırlığına (3g) bağlı olarak %30'dan %70'e değiştirilmiştir. Mekanik ve kimyasal testten sonra, bu bakış açısıyla, öncü mekanik özellikleri nedeniyle ileri analiz için altı TPN filmi seçildi. Genel olarak, %30 ve %40 toplam plastikleştirici içeren TPN Filmler, %50, %60 ve %70 toplam plastikleştiriciler içeren filmlere kıyasla daha yüksek çekme mukavemeti, Sertliğine ve elastik modül değerleri sunmuştur. Eşit toplam plastikleştiricilere sahip TPN filmlerinde sorbitolün gliserole oranındaki artış daha yüksek dansite değerine ve termal stabiliteye yol açmıştı, ancak TPN filmlerinin nem emilimini ve hidrolitik bozunma oranını azalttı. %60 (20S-40G), %50 (20S-30G) ve %40 (10S-30G) plastikleştirici içeren üç grup film, normal insan dermal fibroblast hücrelerinin canlılık analizinin sonuçlarından hücre yapışması ve çoğalması için daha yüksek biyouyumluluk ve uygun yüzeyler sundu. Genel olarak, TPN filmleri daha düşük plastikleştirici yüzdelerinde daha iyi mekanik ve fiziksel özellikler gösterdi, aksine, hücre konusunda, plastikleştiricilerin yüzdelerindeki bir artış, daha yüksek hücre yapışmasına ve canlılığına yol açtı, dolayısıyla TPN filmlerinin biyouyumluluğunu arttırdı.

Anahtar kelimeler: Nişasta, D-Sorbitol, gliserol, Termoplastik nişasta, Normal insan dermal fibroblast hücreleri, Doku mühendisliği

ACKNOWLEDGMENTS

I would like to express my deepest gratitude to my supervisor **Prof. Dr. Menemşe Gümüşderelioğlu** for her kind guidance, advice, criticism, encouragement, and insight throughout the research. Without her vision and ambition, this study would not have been possible.

I would also like to thank **Elvan Konuk Tokak** for her valuable suggestions, comments and support. Many thanks to my lab friends specially **Hazal Şatır,** the person with whom I spent the most beautiful moments.

Finally, I am very grateful to the jury for giving me their precious time. I hope that the research done in line with my master's thesis will be accepted by the honorable professors so that it can be used as a reference for future research.

Here, I would like to thank my parents who have always supported me and dedicate this thesis to them.

TABLE OF CONTENTS

LIST OF TABLES

LIST OF FIGURES

LIST OF ABBREVIATIONS AND SYMBOLS

Symbols

Ca^{++}	Calcium
Mg^{++}	Magnesium
T_d	Degradation temperature
t_d	Doubling time
T_M	Melting temperature
v/v	Volume per volume
w/v	Weight per volume

Abbreviations

3D	3-dimensional
ATR	Attenuated total reflectance
BSA	Bovine serum albumin
DAPI	4, 6-diamidine-2-phenylindole
DPBS	Dulbecco's phosphate buffer solution
DSC	Differential scanning calorimetry
ECM	Extracellular matrix
EthD-1	Ethidium homodimer-1
FBS	Fetal bovine serum
FDA	Food and drug administration

G	Glycerol
g	Gram
h	Hour
HA	Hydroxyapatite
HDPE	High-density polyethylene
HMDS	Hexamethyldisilazane
MTT	3-[4, 5-dimethylthiazol-2-yl]-diphenyl tetrazolium bromide
Min	Minute
n-HDF	Normal human dermal fibroblast cells
PCL	Polycaprolactone
PBS	Phosphate buffered saline
PLA	Polylactic acid
PP	Polypropylene
PS	Polystyrene
P/S	Penicillin/streptomycin
SEM	Scanning electron microscopy
S	D-sorbitol
TE	Tissue engineering
TGA	Thermogravimetric analysis
TPS	Thermoplastic starch
TPN	Termoplastik nişasta
WCA	Water contact angle
XRD	X-ray diffraction

1. INTRODUCTION

The presence of natural polymers as biomaterials has had a desirable efficacy on the development and progress of medical science research [1]. Starch is a natural polymer that is abundant in nature, cost-effective, biodegradable, biocompatible, and non-toxic that has been recognized as a biomaterial with potential to use in tissue engineering and pharmaceutical various fields of experiments [2-4].

Starch is mostly produced in the tubers, roots, seeds, and stems of higher plants, and in few amounts by some mosses, bacteria, protozoa, ferns, and algae [5, 6]. The mixture of two glucose polymers (α-glucans) including amylose, amylopectin together with very small quantities of lipids, water, proteins, and minerals form the semi-crystalline structure of the starch granules in the plants' amyloplasts and chloroplasts [7-9]. Approximately, common starches from different sources of plants and geographical conditions, consist of 70-80% multi-branched amylopectin and 20-30% linear amylose molecules [10]. It is notable that amylose content affects the physicochemical properties of starch [11]. Starch granules have a variety of sizes and shapes depending on their botanical source for example wheat starch granules have lenticular shapes and consist of small and large size types, with an average diameter of 4 and 14 μm respectively [11].

Numerous hydrogen bonds amongst starch macromolecules make starch decompose, before reaching the melting point, under rising temperature conditions. This property can limit the usage of starch. During the hydration of starch by the water as the most common plasticizer, swelling of granules occurs. If the event simultaneously happened by heating starch to about 60-80°C (depending on the source of starch), irreversible swelling and melting of the crystalline region in granules is predictable. The mentioned phenomenon is known as the gelatinization process [12]. Starch conversion to TPS is possible via diverse processes, such as various casting methods, extrusion, blowing, etc., different situations of research, however by modifying starch to thermoplastic starch (TPS), the mentioned problem can almost be solved [12, 13]. Conversion of starch to TPS composites, lead to changes in raw starch's physical, chemical, mechanical, and functional abilities. Starch granules in the presence of water, heat, and shear condition by mixing with plasticizers like glycerol and sorbitol which are approved by the Food and Drug Administration (FDA), undergo disruption, which causes a homogeneous melt named TPS [12, 14].

The source of starch, the type and the amounts of plasticizers selected for fabricating the TPS films influence their mechanical and chemical properties which can presumably play an important role in the interaction of cells with the TPS films. This issue needs further research to select suitable conditions for TPS production that can be used in biomedical applications. Wheat starch is an expensive, accessible, and non-toxic biodegradable natural polymer. In addition, with its high amylose content, it has higher tensile strength than other starch sources. With these properties, it is possible to use wheat starch in biomedical applications. However, it has limitations such that hydrogen bonds between starch molecules cause the starch to deteriorate with increasing temperature. In order to overcome these limitations, in this study, wheat starch was converted into thermoplastic form by using FDA-approved hydrophilic glycerol (G), and D-sorbitol (S) plasticizing agents together. It is aimed to control mechanical properties such as starch retrogradation, plasticizer migration, water resistance and brittleness by using different plasticizers together in the production of TPS.

In this study, the synergistic effect of D-sorbitol and glycerol in the production of wheat starch-based TPS to be used in biomedical applications, especially in tissue engineering was investigated for the first time by mechanical, thermal, chemical, morphological, and crystallographic analyzes. In case of acceptable results, TPS due to its thermoplastic property can be introduced as a candidate biomaterial for utilizing novel technology, 3-dimensional (3D) printing to fabricate scaffolds and patches for application in biomedical and pharmaceutical fields of research.

2. GENERAL INFORMATION

In this part of the thesis, literature information related to the topic of the thesis has been discussed. Firstly, the physical, chemical, and thermal properties of starch polymer and granules from different botanical sources have been discussed. Secondly, information about TPS and their fabrication with different methods and the effects of D-sorbitol and glycerol as plasticizers are mentioned. Lastly, the character of human fibroblastic cells has been mentioned.

2.1.Polysaccharide-Based Natural Polymers

Polysaccharide-based natural polymers presented a high performance in tissue engineering, pharmaceutical, and biomedical research in recent years. Biomaterials are important because traditional materials cannot meet the needs of modern medical studies. Traditional materials were used because they are biologically safe, while biomaterials have a high biological ability to interact with cells and tissues, which is a great selection for advancing medical in vivo fields of research. Natural polymers exhibit extracellular matrix -like properties and, because they are naturally versatile, have led to the development and fabrication of new materials. Polysaccharides like cellulose, chitosan, and starch are available from abundant natural sources and have sufficient biocompatibility and biodegradability properties for use in biomedical applications [15].

Cellulose is a kind of polysaccharide, which is the most abundant biopolymer in the world. This polymer, which is produced in plants and some bacteria, shows significant biochemical and mechanical properties [16, 17]. Nanocelluloses, which are a combination of cellulose extract with nanostructured materials, are used in biomedical research [18]. For example, nanocelluloses are used as scaffolds in tissue regeneration, lesions repair, and as wound dressing. Nanocellulose-based materials have a very high potential in the fabrication of artificial vessels due to their high biocompatibility. Also, in the field of medicine, nanocelluloses presented a good performance in drug delivery [15].

Chitosan is one of the most abundant natural polymers and is a kind of polysaccharide in the world, which is a derivative of chitin and has always been considered due to its high application potential in tissue engineering research. Chitosan-based materials have the ability to delivering of molecules and drugs and have always been considered for their good biodegradability and anti-tumor effects [19].

2.2.Starch

Starch as a polysaccharide is a natural polymer that is abundant in nature, cost-effective, biodegradable, biocompatible, and non-toxic that has been recognized as a biomaterial with the potential to use in tissue engineering and pharmaceutical various fields of experiments [2-4]. Starch is mostly produced in the tubers, roots, seeds, and stems of higher plants, and in few amounts by some mosses, bacteria, protozoa, ferns, and algae [5, 6]. Plants including corn, wheat, potato, and rice are more accessible sources for the production of starch in the world [10]. To get more insight into starch, attention to its physical structure and chemical properties is necessary. The mixture of two glucose polymers (α-glucans) including amylose, amylopectin together with very small quantities of lipids, water, proteins, and minerals form the semi-crystalline structure of the starch granules in the plants' amyloplasts and chloroplasts [7-9].

2.2.1. Amylose and Amylopectin

To know more about starch, it can be important to pay attention to the structure of amylose and amylopectin polymers in detail which form starch macromolecule. Amylose has a linear structure and in some amyloses, this structure is slightly branched. In both groups of these amyloses, it should be noted that the chains are very long and are composed of glucose monosaccharides [19, 20]. However, comparatively, with amylose, the structure of amylopectin is highly branched with short chains. In both of these molecules, glucose molecules bond together with α- (1, 4) glucosidic linkages in linear structure, while α- (1, 6) - glucosidic linkages are formed between glucose molecules to create branched chains [19, 20]. Chemical structure of the amylose and amylopectin is presented in Figure 2.1.

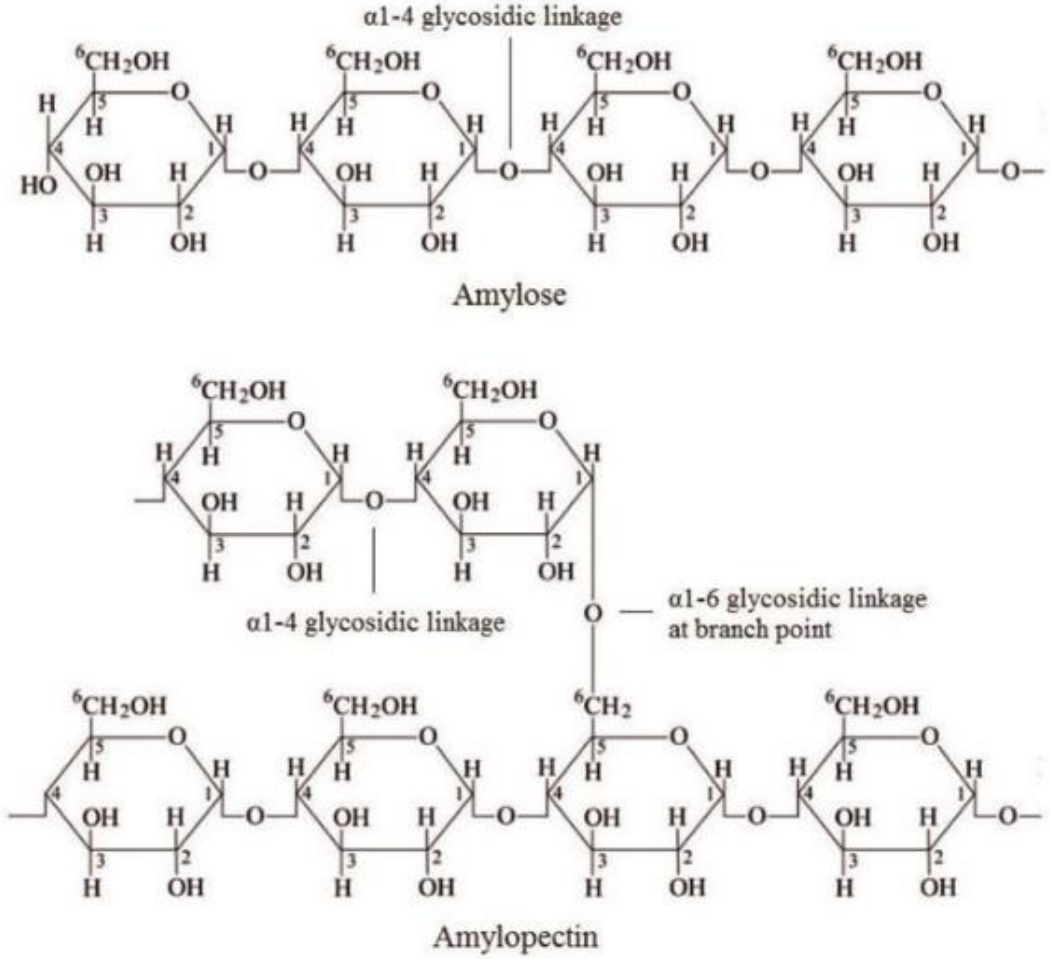

Figure 2.1. Chemical structure of the amylose and amylopectin [20].

Approximately, common starches from different sources of plants and geographical conditions, consist of 70-80% multi-branched amylopectin and 20-30% linear amylose molecules and respectively, have mean molecular masses of 10^6 –10^7 and 10^5g mol^{-1} [11, 19]. Wheat and corn starch with approximately 24.65% compared to potato and rice starch have the highest amount of amylose content among more accessible sources for the production of starch in the world. It should be noted that geographical conditions and plant origins can influence this amount. It is notable that amylose content affects the physicochemical properties of starch [11]. Table 2.1 presented the amount of amylose and amylopectin in starches from different sources.

Table 2.1. Amount of amylose and amylopectin in starches from different sources [21].

Type of starch	Amylose (%)	Amylopectin (%)
Corn	17-25	75-83
Potato	17-24	76-83
Rice	15-35	65-85
Cassava	19-22	28-81
Wheat	20-25	75-80
Waxy	<1	>99
Amylomaize	48-77	23-52

2.2.2. Granule's Morphologies and Sizes

Starch granules have a variety of sizes and shapes depending on their botanical source. For example, corn starch granules have angular shapes and their diameters are mainly between 10 to 24 μm. Wheat starch granules have lenticular shapes and consist of small and large size types, with an average diameter of 4 and 14 μm, respectively. Potato starch granules have a very large diameter of up to 100 μm, while rice starch granules have a much smaller diameter of about 6 μm. It is noteworthy that some research has shown that the diameter of rice granules has a wider dispersion in size. Furthermore, potato and rice starch granules are oval and angular, respectively [11, 19]. The size of starch granules is very important in water absorption because small granule sizes have more surface area and pores in comparison with bigger ones relative to total volume, which causes more water uptake. The more the starch granules are exposed to hydration, their gelatinization, and swelling ability increase [22].

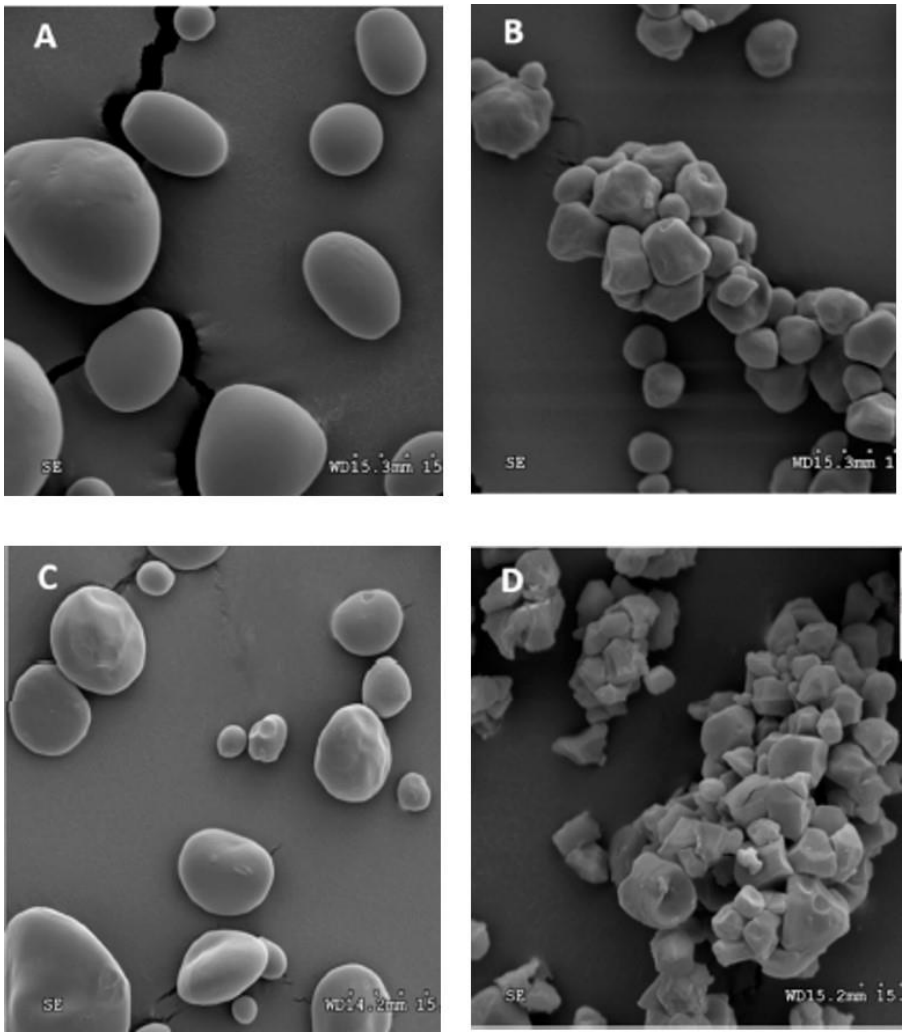

Figure 2.2. SEM micrographs of (A) potato starch (1000X), (B) corn starch (1000X), (C) wheat starch (500X), and (D) rice starch [11].

2.2.3. Crystallinity of Starch

Starch granules have amorphous and semi-crystalline regions. Linear amylose chains and branched segments of amylopectin form amorphous parts of the starch granules, however, double helices of the amylopectin form crystalline parts of the starch. Amylose chains are interspersed among with amylopectin [23]. According to the results of the XRD test of starch granules from different sources, double helixes form three types of crystalline polymorphs. Depending on the source of starch, granules presented different crystallinity types which can be A, B or both of them named type C. Form A has a monoclinic unit cell and form B has a hexagonal unit cell [24]. There are channels in type B crystalline lattices that fill up with water, while in type A, these channels do not exist [25]. (See Figure 2.3). In ordinary and high amylose starches, crystalline content is less than in waxy starches. Cereal starches like rice, and wheat presented A-type crystallinity However B crystallinity structure mostly is in

high amylose starches which are stored in fruits, tubers, and stems of the plants [25]. Table 2.2 presented the amount of crystallinity and its type from different sources of starch.

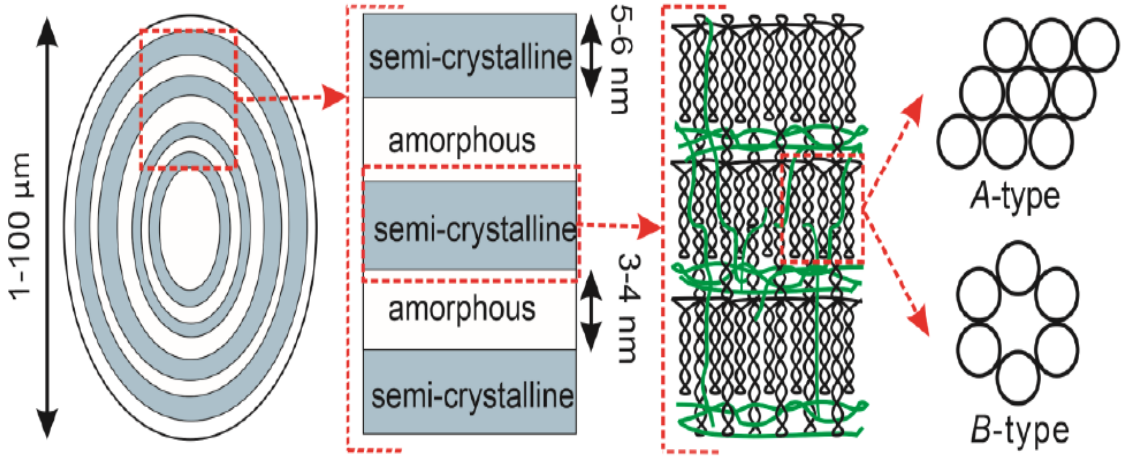

Figure 2.3. A graphical illustration of starch structure [23].

Table 2.2. The crystallinity degree of starch obtained from different sources [25].

Source of starch	Crystallinity (%)	Crystallinity type
Corn	14-39	A
Wheat	27-36	A
Waxy rice	~38	A
Potato	23-25	B
Banana	18–22	B
Cassava	~13	C
Tapioca	35-38	C

2.2.4 Gelatinization Process of Starch

Many parameters such as temperature, water content, pressure, structure, and starch source affect the interaction of water with starch molecules. Temperature plays an essential role in water interaction with starch granules because, at low temperatures, molecules that have an amorphous structure absorb water and swelling occurs, however, in the case of drying of this

suspension, this is a reversible process. But at higher temperatures this phenomenon is irreversible. But the amount of water used is very important if this amount is more than 60% (w/w), this phenomenon is called gelatinization (irreversible). In the gelatinization of starch, the crystalline regions of the granules also melt and the structure of the molecules and granules of the starch is disrupted and solubilization in water also occurs [26]. It is noteworthy that when the temperature rises, the water first affects the amorphous regions of the granules, where the first swelling occurs, but this event causes forces to destroy the crystalline regions, and eventually, the polysaccharide which is soluble in the water obtained [26]. Amylose and amylopectin are responsible for gelling and viscosity of starch in water, respectively [27]. The gelatinization temperature also varies according to the source of starch, which can be seen in the Table 2.3.

Table 2.3. Gelatinization temperatures of common types of starch.

Source of starch	Gelatinization temperature	REF.
Corn	62-80	28
Waxy Corn	63-72	28
Potato	58-65	28
Tapioca	52-65	28
Barley	52-85	28
Wheat	51-60	28

2.2.5. Retrogradation Process of Starch

In gelatinized starch, after passing time and cooling, some of the molecules of amylose and amylopectin recrystallize due to the migration of moisture from the gel network, which is called the retrograde phenomenon. In this phenomenon, very strong re-associate hydrogen bonds are created between the amylose [25, 30].

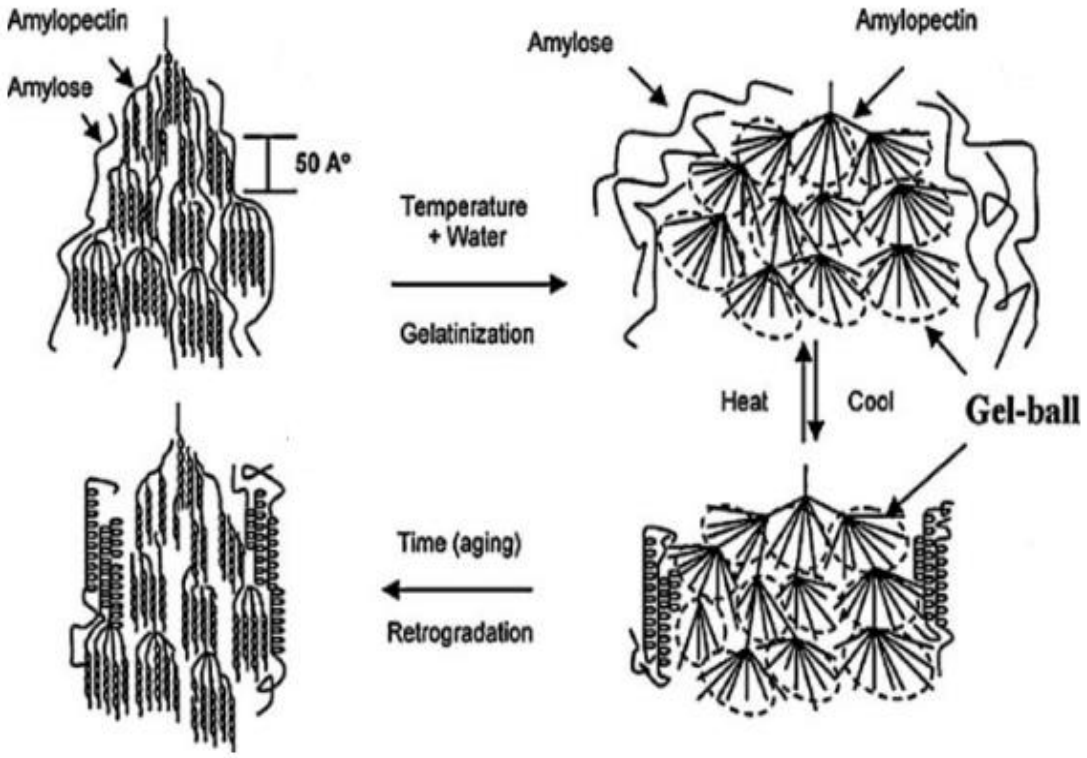

Figure 2.4. Schematic representations of starch gelatinization and retro-gradation [31].

2.3. Thermoplastic Starch

According to the potentials of starch, numerous hydrogen bonds amongst starch macromolecules make starch decompose, before reaching the melting point, under rising temperature conditions. This property can limit the usage of starch in different situations of research, however by modifying starch to thermoplastic starch, the mentioned problem is nearly solvable [12, 13]. Conversion of starch to TPS composites, lead to changes in raw starch's physical, chemical, mechanical, and functional abilities. Starch granules in the presence of water, heat, and shear condition by mixing with plasticizers like glycerol and sorbitol which are approved by the Food and Drug Administration (FDA), undergo disruption, which causes a homogeneous melt named TPS [12, 14]. During the hydration of starch by the water as the most common plasticizer, swelling of granules occurs. If the event simultaneously happened by heating starch to about 60-80°C (depending on the source of starch), irreversible swelling and melting of the crystalline region in granules is predictable. The mentioned phenomenon is known as the gelatinization process [12].

Furthermore, using just water as a plasticizer cannot submit desired properties in obtained TPS. Therefore, using hydrophilic plasticizers such as glycerol, sorbitol, or other types of plasticizers like xylitol, maltitol and urea can enhance the thermo-plasticity property of TPS,

by penetrating the starch granules [12, 32]. In general, the reason for modifying starch is to be able to improve its mechanical and thermal properties and minimize its crystallinity, as well as increase its resistance to oxygen and moisture.

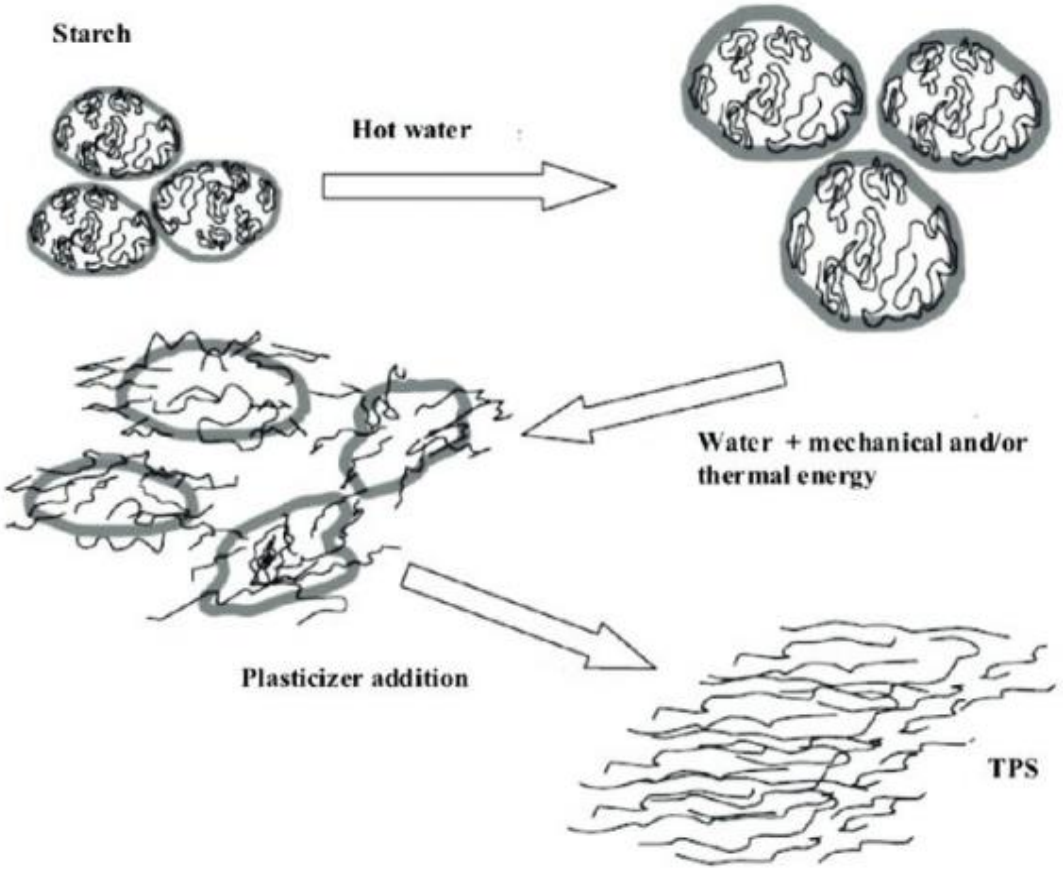

Figure 2.5. Gelatinization and plasticization of starch [33].

2.3.1. Effect of Glycerol and D-sorbitol in TPS Fabrication

Sorbitol and glycerol can be a good choice as a plasticizer due to their FDA approval and strong ability to interact and establish hydrogen bonding with starch. The use of multiple plasticizers such as sorbitol and glycerol can prevent or reduce starch retrogradation, migration of plasticizers, fragility, glass transition temperature and also can control water resistance and mechanical properties of TPS. Sorbitol as a plasticizer of TPS has advantages and disadvantages over glycerol. Due to the higher melting temperature of sorbitol (95°C) than glycerol (18°C), the volatility of the TPSs is reduced and a stronger bond between sorbitol and starch reduces the water absorption of the films, which increases the water resistance of TPSs. Furthermore, Sorbitol increases the decomposition temperature of TPS compared to glycerol-plasticized TPS. Over time, sorbitol can increase the brittleness and recrystallization of TPS due to its migration to the TPS surface. However, to prevent this

problem, glycerol can be used, which approximately improves the properties of TPS films [14, 34]. Sorbitol and glycerol molecular structure presented in Figure 2.6.

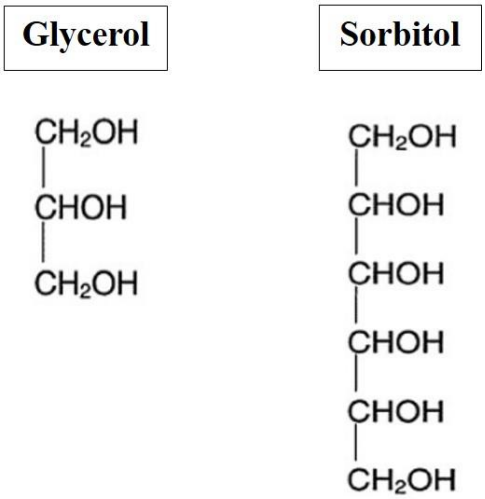

Figure 2.6. Sorbitol and glycerol molecular structure [35].

2.3.2. Thermoplastic Starch Fabrication Methods

Starch conversion to TPS is possible via diverse processes, such as various casting methods, extrusion, blowing, and etc. which are briefly discussed below [12].

2.3.2.1. Solution Casting Methods

The solution casting method is mainly used for laboratory experiments in fabricating TPS films to study the mechanical and thermal properties of them. In this method, materials such as starch, plasticizers, and other additives added to the water. As the temperature rises to a certain extent, the starch granules become gelatinized and the plasticizers penetrate well into the granules. Then, after a certain period of time, the produced suspension is cooled and poured into a petri dish, etc. And is kept at a certain temperature until the water in the suspension evaporates completely and the solution dries. Then the films were separated from the platform and the TPS films obtained [36-38]. Figure 2.7 presented solution casting procedure. It should be noted that in this procedure, respectively, the amount of temperature and time to prepare the TPS solution is very important [38].

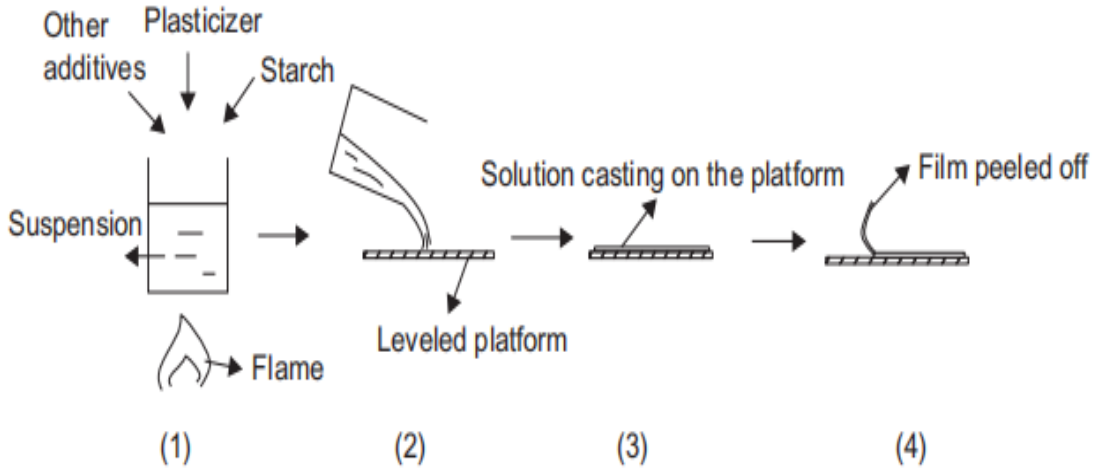

Figure 2.7. Solution casting procedure to fabricate TPS film: (1) Starch solution producing and heating. (2) Casting the obtained solution on to a platform. (3) Cooling and drying. (4) Peeling the dried film off of the platform [38].

2.3.2.2. Extrusion

Extruders are commonly used in the production of large quantities of TPS in the industry. A typical extruder with a single-screw consists of components such as a die, barrel, screw, etc. which is presented in Figure 2.8. TPS production with the extrusion procedure begins by adding materials such as starch, plasticizers, etc. Inside the extruder, high shear force and temperature are applied to the material, which destroys the crystallinity of the starch and mixes the material together. In fact, the hydroxyl groups of starch interact with the water inside the plasticizers and starch. The starch melts and creates a homogeneous paste of the material inside the extruder. At the end of this processor, the extruder breaks the obtained TPS into pallets (see Figure 2.9), which can then be re-inserted into the extruder with other polymers or other materials. TPS pellets are melted inside the extruder and mixed with other polymers and additives. The TPS paste that comes out of the extruder solidifies very quickly. In order to be able to shape the produced TPS into different forms, when TPS comes out of the extruder, films or sheets can be produced by the blowing method (see Figure 2.10), or they can be molded to any shape [37-41].

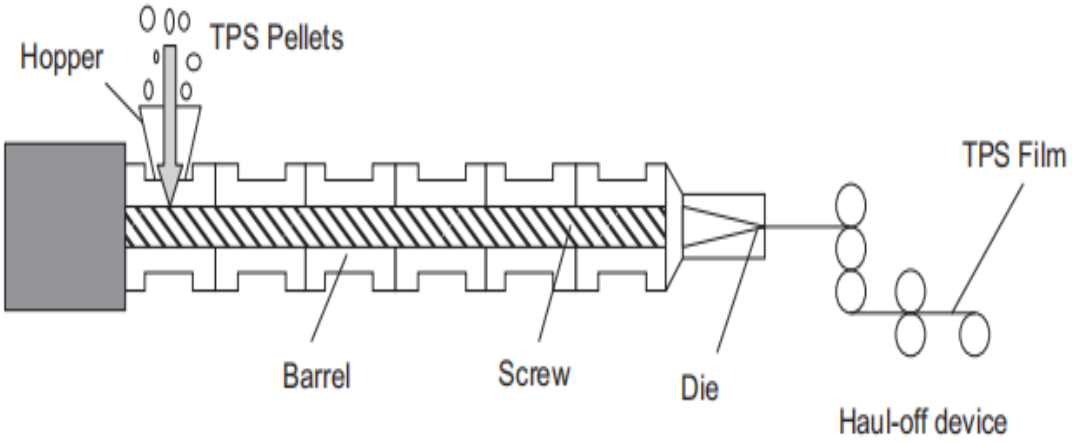

Figure 2.8. A schedule of a typical extruder and extrusion processing [38].

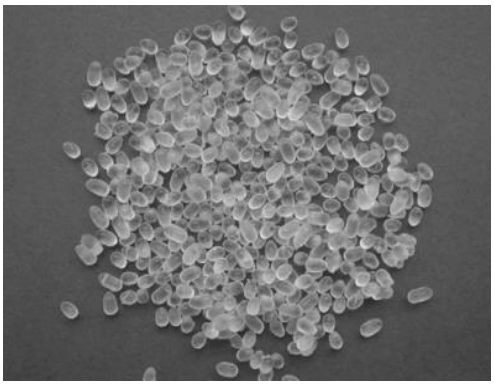

Figure 2.9. Pellets of potato starch containing 25% glycerol [38].

Figure 2.10. TPS film blowing [38].

2.3.3. Impact of Starch Source on TPS Films

The source of starch has a significant effect on the physicochemical properties of fabricated TPS films due to the amount of amylose and amylopectin. Recently, research about TPS films that are fabricated by the solution casting method from four sources of starch including potato, wheat, corn and rice, with glycerol as a plasticizer has been conducted. Due to their higher amylose content, respectively, wheat and corn starch TPS films had the best resistance with higher tensile strength and young's modulus but presented the lowest stretch ability. Conversely, rice TPS films due to their highest molecular weight and amorphous properties presented higher elongation at break and the lowest tensile strength and young's modulus. TPS films of the potato starch due to their medium molecular weight and crystallinity had shown intermediate mechanical properties in comparison with TPS films' of other sources [11]. Amylose and amylopectin have different sensitivities to plasticizers. Research has shown that starches that have more amylopectin interact more with plasticizers and this property makes the effect of plasticizers on the flexibility and extensibility of TPS films more obvious. In one study, TPS films were produced from ahipa, cassava, and corn starch. Films made from ahipa starch showed more interaction with plasticizers due to having more amylopectin, which has the ability to establish more hydrogen bonding than amylose [38].

2.3.4. Reinforcement of TPS products

TPS films are not water-resistant and maybe cannot present suitable mechanical and thermal properties. For this reason, its properties can be improved by mixing TPS with other polymers and mineral materials [12]. TPSs have two obvious drawbacks due to their high water sensitivity and weakness in mechanical properties, but these shortcomings can be partially improved by blending TPSs with other polymers, fibers, different types of plasticizers, and other additives. Studies have shown that biodegradable and non-biodegradable polymers such as high-density polyethylene (HDPE), polypropylene (PP), polystyrene (PS), polylactic acid (PLA), and polycaprolactone (PCL) blended with TPS in compared to TPS, showed higher tensile strength and elastic modulus. Research has shown that fibers increase the mechanical properties and water and thermal resistance of TPS due to their good ability in establishing hydrogen bonding with starch. However, it should be noted that the amount of fibers used in TPS is a very important parameter because in disproportionate amounts, instead of improving the properties of TPS, they act in reverse due to their agglomeration in the composite. Cellulose nanocrystallites and cellulose fibers are the examples used for the reinforcement of TPS properties [38].

2.4. Human Fibroblast Cells

The most abundant connective tissue cells in the human body are fibroblast cells, which are mesenchymal derived. It is a notable cellular process in fibroblast cells that is very extensive. These cells play an essential role in the physiological process such as forming the extracellular matrix (ECM), regularities in wound healing, tissue repairing, and secretion of growth factors, cytokines and, epidermal proliferation and differentiation [43]. The fibroblasts in the skin are located in the dermis area, and the ECM produced by these cells is rich in collagen. When the skin gets a wound or scar, these cells play a very important role in its repair [44]. Typical human Fibroblast cells are spindle-shaped and elongated. These cells had an oval or round nucleus in the center of the cell [42]. Fibroblast cells are accessible throughout the human body in connective tissues, which can be seen as examples of harvested fibroblast cells in Figure 2.11.

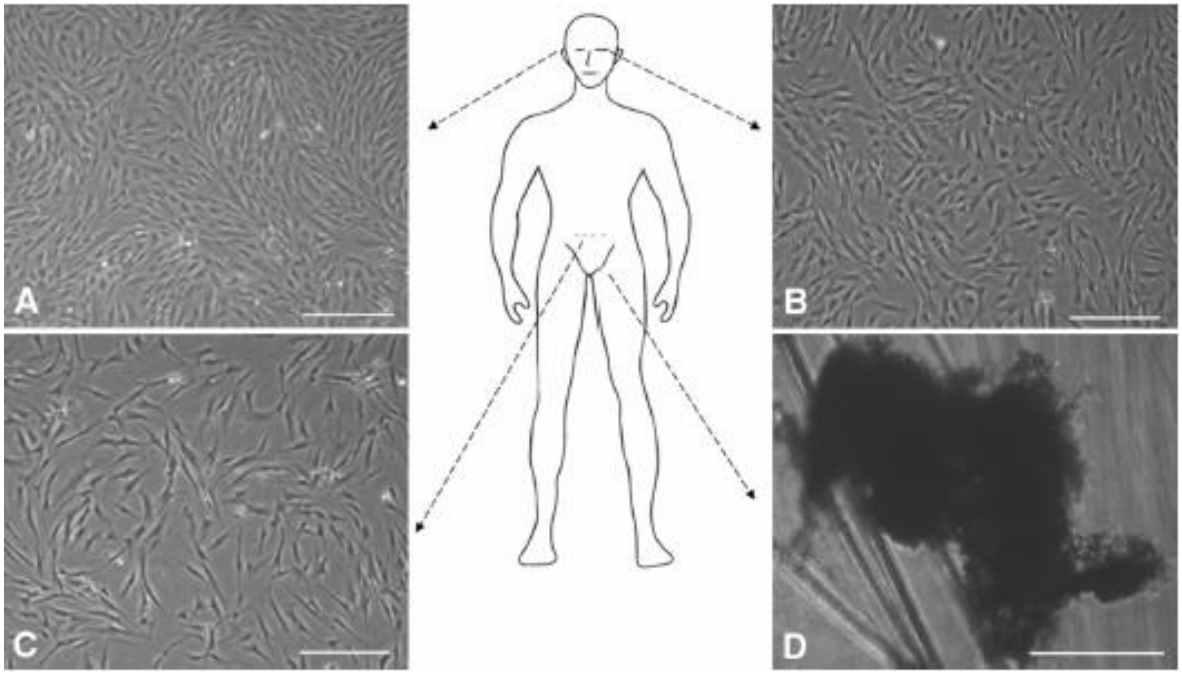

Figure 2.11. Body sites selected for the harvesting of fibroblast cells: A) Fibroblast cultured from the back of the ears (otoplasty) and, B) fibroblast cultured from Eyelid (blepharoplasty), C) fibroblast cultured from Cesarean Scar (abdomen) e, D) Skin tissue from Groin under cell culture conditions, which did not spread cells [43].

2.5. Application of Starch and TPSs in Biomedical Research

Starch-based biomaterials bring significant improvements in different biomedical research by utilizing various methods. For example, electrospun Starch-Polyhydroxybutyrate scaffolds represent preferable properties for bone tissue engineering research. Due to the attendance of starch, increment in tensile strength, biodegradation, hydrophobicity and cell viability ability of PHB-starch scaffolds was dramatically visible [45]. Another material that is used widely in the scope of bone tissue engineering is hydroxyapatite. However, Scaffolds of HA-composites, because of their hardness and brittleness cannot produce fruitful results. The binder ability of starch in gelatinized phase with HA-composites permits utilizing one of the novel technologies, 3D printing, to fabricate scaffolds and lead to an increase in the tensile strength of fabricated scaffolds. Which is very close to the mechanical properties of the cancellous part of the bone tissue, and causes an increment in the bioactivity of scaffolds [46]. Recently, a biomaterial consisting of N, O-carboxymethyl chitosan, and starch, was developed and 3D printed as scaffolds for application in wound healing and dressing. The ability of starch in changing the degradation rate and drug-releasing properties of the biomaterial was the significant aim of using starch in this research [47]. Moreover, starch in the pharmaceutical industry plays an important role in diluting and disintegrating capsules and tablets and is known as an excipient and a binder. In addition, the ability of starch as micro and nanoparticle in delivering specific molecules and drugs to specific areas of the body to treat some diseases is notable [48-50]. To evaluate the biocompatibility of starch thermoplastic films for biomedical applications, a study was performed by implantation of 3T3 fibroblast cells. The results showed that TPS films of andean starch had good biocompatibility, however, cell adhesion ability on this film needed promotion [51].

3. MATERIALS AND METHODS

The aim of this study is to fabricate thermoplastic wheat starch films with different ratios of plasticizers to evaluate the biocompatibility of these materials and selected the best choices for biomedical applications and use in tissue engineering. First, the characteristics of wheat starch used in the experiment were investigated. Secondly, starch thermoplastic films were made with a total of 30 to 70 percent of plasticizers with different ratios of D-sorbitol and glycerol by solution casting methods. Thirdly properties including pH and viscosity of TPS solution were measured. Fourth, mechanical, physical, temperature, and chemical tests were conducted to investigate and characterize the films and the best films were selected for further research in cell culture experiments. And in the last part, cell studies were done by culturing normal human dermal fibroblast cells and the best groups were introduced for further research.

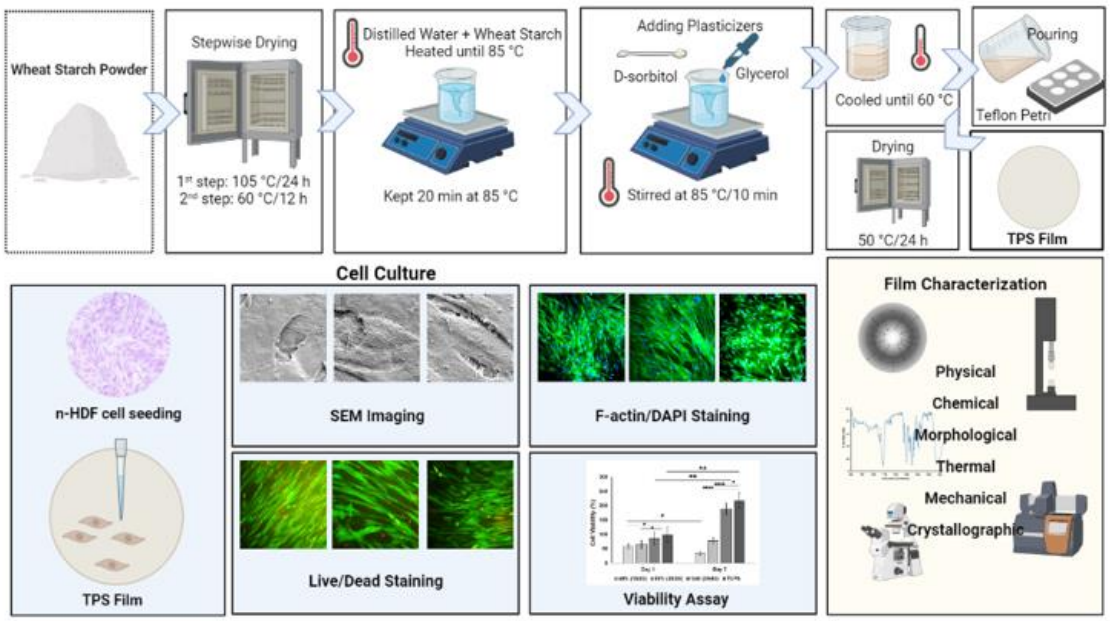

Figure 3.1. Briefly, experimental studies performed within the scope of thesis.

3.1. Materials

Wheat, rice and corn starch was obtained respectively from Yazar Company, (Turkey), Yazgan company (Turkey) and Alfasol Company (Turkey). The plasticizers used in this study D-sorbitol with 97% purity and Glycerol with ≥98% purity respectively provided by Acros Organic, (Belgium) and ISO-LAB Chemicals, (Germany). Wheat starch was dried respectively at 105°C for 24 h, and at 60°C for 12 h, before using in the test case. Sodium azide that was used in the hydrolytic degradation analysis of the films, was purchased from Sigma Aldrich (Germany).

For cell culture studies Normal human dermal fibroblast (n-HDF) primary cells were supplied from Hacettepe University Center for Stem Cell Research and Development (PEDI-STEM) (Turkey). For culture medium, Low glucose DMEM was supplied from Capricorn Scientific (Germany). Additionally, L-glutamine, fetal bovine serum (FBS) and penicillin/streptomycin (P/S), Dulbecco's phosphate buffer solution (DPBS) were obtained from Biowest (USA). Phosphate buffered saline (PBS) tablets (pH: 7.4), 3-[4, 5-dimethylthiazol-2-yl]-diphenyl tetrazolium bromide (MTT), Glutaraldehyde solution (25%, v/v), Hexamethyldisilazane (HMDS), Bovine serum albumin (BSA), Trypsin-EDTA solution, crystal violet and Ethidium homodimer-1 (EthD-1) and Calcein AM were supplied from Sigma-Aldrich company (Germany). Triton X-100 was provided from Merck (Germany). Alexa Fluor® phalloidin 488 and 4, 6-diamidine-2%-Phenylindole (DAPI) were provided from Invitrogen (USA).

3.2. Raw Wheat Starch Moisture Evaporation Percentage Measurement During Drying

To calculate the moisture content of the wheat starch, firstly, 10 g of it in powder case were dried for 24 and 12 h at 100°C and 60°C in an oven, respectively. Then the weight of dried starch was measured. The moisture content of starch was calculated using the following formula:

$$MC\ (\%) = \frac{(W_1 - W_2)}{W_1} \times 100 \quad (1)$$

In Equation 1, W_1 is the initial weight of the raw wheat starch and W_2 is the dried weight of it.

3.3. SEM Analysis of the Raw and Dried Wheat Starch Granules

To study the surface morphology and sizes of the raw and dried wheat starch granules SEM analysis was conducted, Firstly, samples surfaces were coated with gold-palladium, and then the test was performed at different magnifications using the SEM (Tescan, FIB-SEM, GAIA3, Czech Republic). By using SEM micrographs granule sizes were measured with Image J Software (NIH, Bethesda, MD).

3.4. Gelatinization and Solubility of Starch Granules from Different Sources

To observe gelatinization and solubility of starch granules in excess water at an increasing temperature condition, 3 g of starch from different sources (rice, wheat, or corn) was added in 100 mL and their behavior and morphologies changes were observed by increasing the water temperature with a confocal microscope at 25°C, 55°C, and 85°C.

3.5. Film Fabrication

The solution casting scheme is the method that was utilized for film preparation. In the first stage, the mixture of 100 mL autoclaved distilled water and 3 g wheat starch was heated until 85°C ± 2°C with continuous stirring at 105 rpm, afterward, the mixture was kept at that temperature for 20 min. In the next stage by adding plasticizers, that include glycerol and D-Sorbitol, the mixture was stirred at a constant temperature of 85°C ± 2°C for ten minutes, then the solution was cooled until 60°C. Lastly, 10 mL of the mixture was poured into the petri dishes with 5 cm diameter, afterward, the petri dishes were put in the oven for 24 h at 50°C to dry up the solution. The plasticizers portion of the films was altered from 30% to 70% depending on the starch weight (3 g) and different ratios of D-sorbitol and glycerol were used in each percentage which is presented in Table 3.1.

Table 3.1. The amount of plasticizers used to fabricate each group of TPS films.

Film Name	Total Plasticizer		D-Sorbitol		Glycerol		
	%	(g)	%	(g)	%	(g)	(mL)
10S20G	30	0.9	10	0.3	20	0.6	0.48
20S10G	30	0.9	20	0.6	10	0.3	0.24
10S30G	40	1.2	10	0.3	30	0.9	0.72
20S20G	40	1.2	20	0.6	20	0.6	0.48
30S10G	40	1.2	30	0.9	10	0.3	0.24
10S40G	50	1.5	10	0.3	40	1.2	0.96
20S30G	50	1.5	20	0.6	30	0.9	0.72
30S20G	50	1.5	30	0.9	20	0.6	0.48
40S10G	50	1.5	40	1.2	10	0.3	0.24
10S50G	60	1.8	10	0.3	50	1.5	1.2
20S40G	60	1.8	20	0.6	40	1.2	0.96
30S30G	60	1.8	30	0.9	30	0.9	0.72
40S20G	60	1.8	40	1.2	20	0.6	0.48
50S10G	60	1.8	50	1.5	10	0.3	0.24
10S60G	70	2.1	10	0.3	60	1.8	1.44
20S50G	70	2.1	20	0.6	50	1.5	1.2
30S40G	70	2.1	30	0.9	40	1.2	0.96
40S30G	70	2.1	40	1.2	30	0.9	0.72
50S30G	70	2.1	50	1.5	20	0.6	0.48
60S10G	70	2.1	60	1.8	10	0.3	0.24

3.5.1. Wheat TPS Solutions' Viscosity Analysis

The viscosity measurements of the TPS solutions with different total plasticizers and D-sorbitol/glycerol ratios which were used in films fabrications at different temperatures respectively 4°C, 15°C, 25°C, 37°C and 45°C were conducted by using an Engler viscometer. Firstly, the density of the TPS solutions was measured by dividing the mass by its volume of it. Regarding the water density in different temperatures which are 1 g/mL at

4°C and 0.99 g/mL at nearby 6°C to 48°C and the viscosity of the water which are 1.56, 1.13, 0.89, 0.69 and 0.59 mPa.s respectively in 4°C, 15°C, 25°C, 37°C and 45°C the time of the laminar flow rate of the water and TPS solutions were taken in different temperatures by using Engler viscometer. Lastly, the viscosity of the TPS solutions was calculated from the Equation 2 given below.

$$\frac{\mu_{solution}}{\mu_{water}} = \frac{t_{solution}}{t_{water}} \times \frac{\rho_{solution}}{\rho_{water}} \quad (2)$$

3.5.2. Wheat TPS Solutions' pH Analysis

The pH of TPS solutions with different total plasticizers and various ratios of D-sorbitol/glycerol was measured using a pH meter (Mettler Toledo). Tests were repeated at least three times for each sample.

3.6. Film Characterization

3.6.1. Thickness

By using a manual micrometer, the thickness of films in different regions on them was measured at least three times with the nearest 0.01 mm sensitivity.

3.6.2. Density Measurement

For density determination, the TPS films were cut in 2 cm x 2 cm dimensions and dried at 105°C in the vacuum oven for 24 h. Then dried films were weighed. Film densities were calculated by using film thickness and weight (m_{film}) values. Densities of films (ρ) were calculated using the Equation 3 given below.

$$\rho_{film} = \frac{m_{film}}{V_{film}} \left(V_{film} = thickness \times length \times height\right) \quad (3)$$

3.6.3. Moisture Content Measurement

The moisture content of the TPS films was determined by the ASTM D644-99 standard. Therefore, the films were cut into 2 cm × 2 cm pieces, and their weights were measured. Films were kept in the oven at 105°C for 24 h to drying, then their weights were measured again. The moisture content of films (MC) was calculated using Equation 4.

$$MC\ (\%) = \frac{(W_1 - W_2)}{W_1} \times 100 \quad (4)$$

In Equation 4, W_1 is initial weight of the films and W_2 is dried weight of the films.

3.6.4. Water Solubility Analysis

For the determination of water solubility, (WS) of the films were cut into 2 cm × 2 cm pieces, dried in the oven at 105°C for 24 h and their initial weights ($W_{1)}$ were measured. Then the films were immersed in the 10 mL distilled water for 24 h under gentile stirring. Afterward, the films were dried in the oven at 105°C for 24 h in order to measure their finite weight ($W_{2)}$. For the calculations, Equation 5 was used.

$$WS(\%) = \frac{w1-w2}{w1} \times 100 \quad (5)$$

3.6.5. Mechanical Test

According to the ASTM 638 standards scheme, the mechanical properties of TPS films were conducted by Texture Analyzer TA.XTplusC (Stable Micro System, UK). The selected films for the mechanical testing were cut into rectangular pieces of 1 cm width and 5 cm length. Mechanical tests were repeated at least three times for each film group using a load of 0.05 N and a constant crosshead speed of 10 mm/min.

3.6.6. Attenuated Total Reflectance-Fourier Transform Infrared (ATR-FTIR) Analysis

Using the ATR technique, FTIR analysis of dry wheat starch, D-sorbitol, glycerol, and selected TPS films in the wavelength range of 400 cm^{-1} to 4000 cm^{-1} was implemented (Thermo-Scientific Nicolet iS10, USA).

3.6.7. Hydrolytic Degradation Tests

To perform the hydrolytic degradation test, firstly, the films of the selected groups were cut to 1 cm × 1 cm and their initial weight was measured. Secondly, they were immersed in 2 mL falcons containing Phosphate buffered saline (PBS) with a pH of 7.4 and 0.2% (w/v) sodium azide. In this experiment, sodium azide was used to prevent contamination by microorganisms. Thirdly, the samples were kept in the incubator at 37°C with a shaking speed of 50 rpm for 1 week. After one week, the films were dried at room temperature and their weights were measured. Lastly, by subtracting the final weight of each sample from its' initial weight, the amount of hydrolytic degradation was calculated for that film. In this study, at least three samples from each group of the selected films were tested.

3.6.8. Determining Water Uptake Capacities

First, the films of the selected groups were cut to 1 cm × 1 cm sizes, and their initial weights (Wi) were measured. The films were then immersed in PBS with a pH of 7.4 and their weight changes were measured at 0.5, 1, 2, 3, 4, and 24 h after exposure to PBS (W_f). In this experiment, at least three samples were tested for each group of films. The filter paper was also used to absorb excess water from the films before weighing. Water-uptake capacities of films (WC) were calculated using the Equation 6 given below.

$$WC\% = \frac{(W_f - W_i)}{W_i} \times 100 \quad (6)$$

Here, W_f is the mass of the dry films and W_f is the mass of the swollen films after water uptake.

3.6.9. X-Ray Diffraction (XRD) Analysis

By using a radiation source of CuKα in a horizontal diffractometer (Rigaku Ultima-IV, Japan), XRD analysis of the selected films, respectively in scanning range and speed of 5°-35° and 1°/min, was implemented. By using Origin Pro 8.1 software (USA) the XRD patterns of the films were achieved.

3.6.10. Water Contact Angle (WCA) Measurements

Water contact angle measurements of the selected TPS films were performed by the sessile drop (pendant drop) method at room conditions (Biolin Scientific, China).

3.6.11. Film Roughness Analysis

By using a perthometer (Mahr, M2, ABD), the roughness feature of the selected films at room temperature was investigated. This measurement was performed at least four times for each film of selected groups.

3.6.12. Thermogravimetric Analysis (TGA)

To investigate the thermal degradation of dried wheat starch, D-Sorbitol, Glycerol, and selected films, 1 mg of samples were analyzed under a nitrogen atmosphere, utilizing TG/DTA 6300 instrument (Seiko Instruments, USA). The samples were heated from room temperature to 400°C with an increment rate of 10°C/min.

3.6.13. Differential Scanning Calorimetry (DSC) Analysis

To inspect the thermal behavior of dried wheat starch, D-sorbitol, glycerol, and the selected films, by using Diamond DSC (PerkinElmer, USA) instrument, the samples were heated from room temperature to 300°C at the increment rate of 10°C/min, to perform the DSC analysis.

3.6.14. Scanning Electron Microscopy (SEM) Analysis

To study the morphology of the selected films' surfaces, Firstly, their surfaces were coated with gold-palladium, and then the test was performed at different magnifications using the SEM (Tescan, FIB-SEM, GAIA3, Czech Republic).

3.7. Characterization of Normal Human Dermal Fibroblast Cells

For the characterization of Normal Human Dermal Fibroblasts (N-HDF) primary cells obtained from PEDI-STEM, cell count, MTT analysis, F-actin/DAPI staining, and crystal violet staining were performed. The characterization process was continued in the batch culture system for 14 days. Cell seeding inoculation density was chosen as 8×10^3 cells/1.9 cm^2. In this context, approximately 40×10^3 cells/well were inoculated into 6-well cell culture dishes, approximately 8×10^3 cells/well in 24-well cell culture dishes, and approximately 4.7×10^3 cells/well in 48-well cell culture dishes. Cells frozen in passage 8 were opened in a 75-cell culture flask (P9) with an appropriate medium and inoculated at passage 10 when the cells reached 90% confluency. In this characterization, the cell growth medium included 10% FBS, 2% L-glutamine, 1% P/S and DMEM Low glucose. The culture medium added for cell growth for each well in 6, 24, and 48 well culture dishes were 3, 1, and 0.5 mL, respectively.

3.7.1. Cell Count

Cells were counted on the 1^{st}, 2^{nd}, 3^{rd}, 5^{th}, 7^{th}, 10^{th}, and 14^{th} days of the culture, which were removed from the surface by incubating with 0.5 mL of 0.25% trypsin/EDTA solution for 5 min in the 5% CO_2 atmosphere in an incubator (Heraus, Germany). Counting was carried out with 4 parallel wells and 2 times counting for each well. Hemocytometre (Neubauer chamber) was used for counting living cells.

3.7.2. MTT Analysis

MTT analysis was performed on the culture's 1st, 2nd, 3rd, 5th, 7th, 10th, and 14th days to determine cell viability. The medium on the cells was removed and 600 µL of serum-free medium and 60 µL of MTT solution were added to each well. Then, incubation was carried out in the 5% CO_2 atmosphere in an incubator (Heraus, Germany) for 3 h. At the end of the incubation, the medium on the cells was aspirated and 400 µL of isopropanol was added to each well to dissolve the formazan crystals. Two hundred µL of the resulting solution was transferred to 96-well culture dishes. Measurements were conducted by spectrophotometer at 570 nm, with 690 nm as a reference, and the optical densities of the solutions were determined.

3.7.3. Crystal Violet Staining

Examination of the morphology of the N-HDF cells on the 1st, 3rd and 7th day of the culture was conducted by histological staining which was done with crystal violet. The medium on the cells was removed and washed 3 times with PBS. For fixation, cells were kept in acetone/methanol solution for 20 min at 4°C. After fixation, 500 µL of crystal violet solution was added to the cells and incubated for 30 min. The stained surface was washed with water and visualized under an inverted microscope.

3.7.4. F-Actin/DAPI Staining

Visualization of N- HDF cells morphology was performed by F-actin/DAPI staining in 1st and 2nd days of the culturing. Alexa Fluor 488 conjugated anti-F-actin antibody was used to stain the cytoskeleton, and DAPI (4', 6-diamidino-2-phenylindole, dihydrochloride) dye was used to stain the nucleus. On the specified days of culture, the medium on the cells was removed and washed 3 times with PBS. Fixation was performed with 2.5% (v/v) glutaraldehyde for 10 min. After the fixation process, three washes with PBS were done. Then, the cells were incubated in the PBS solution containing 0.1% (v/v) Triton-X-100 for 10 min to increase membrane permeability. After removing the 0.1% (v/v) Triton-X-100 solution, the samples were washed with 1% (Bovine Serum Albumin) BSA/PBS 3 times for 5 min by shaking. Then, 100 µL of F-actin/DAPI was added to each well and incubated for 30 min in the dark, and at the end of this period, the cells were washed again with 1% BSA/PBS solution 3 times for 5 min and staining was completed. Imaging was performed with a fluorescent microscope (Zeiss LSM 510, Germany).

3.8. Cell Culture Studies

3.8.1. Determination of Cell Viability

3.8.1.1. MTT Analysis

MTT analysis in this study was performed for samples in the 1st and 7th days of the culturing. Firstly, the culture medium was aspirated from the wells. Secondly, 60 µL MTT solution and 600 µL serum-free medium were added to each well, and samples were then kept in the 5% CO_2 atmosphere in an incubator (Heraus, Germany) at 37°C for three hours. Thirdly, the solution of the wells was again aspirated, and instead, 400 µL of isopropanol was added to dissolve Formazan crystals. Lastly, with a spectrophotometer (Asys UVM 340, Austria) at 570 nm wavelength, the MTT analysis results were obtained (The reference wavelength was 690 nm).

3.8.1.2. Live/Dead Staining

In the live/dead staining scheme, Ethidium homodimer-1 (EthD-1) was used for the dyeing of dead cells' nucleic acids and Calcein AM dye was used for the detection of live cells in the 1st and 7th day of the culturing. After 3 times washing of the samples with Dulbecco's phosphate buffer solution (DPBS+) (containing Ca^{++} and Mg^{++}) for 30 minutes the samples were incubated in a solution containing DPBS, Ethidium homodimer-1 (EthD-1), and Calcein AM at room temperature. Finally, they have washed again with DPBS and observed under the fluorescent microscope (Zeiss LSM 510, Germany).

3.8.2. SEM Analysis

To study and observed the morphology of n-HDF cells on the films in the 1st and 7th days of the culturing, SEM analysis was performed. In this analysis, after aspirating the culture medium from the wells, the cells were fixed with Glutaraldehyde solution (2.5%, v/v) for 30 minutes. In the next step, to dehydrate the samples, solutions with concentrations of 30%-100% ethanol were used. Additionally, just for 5 min, HMDS was added to the samples and then they dried completely at room temperature. Finally, samples with gold-palladium coat were analyzed by SEM (Tescan, FIB-SEM, GAIA 3, Czech Republic).

3.8.3. Cytoskeleton/Nucleus Staining

On the seventh day of the culturing, to inspect and observe the cytoskeleton and nucleus of n-HDF cells, F-Actin/ DAPI staining was performed. In the first step, the culture medium was aspirated from the wells and the samples were 3 times washed with PBS. The cells were then fixed with 2.5% (v/v) Glutaraldehyde for 10 min. Afterward, samples were washed with PBS, again 3 times, and then kept in 0.1% (v/v) triton-x for 10 min. Then the solution was aspirated from the wells and the samples were washed 3 times with 1% BSA/PBS for 5 min. By adding Alexa Fluor® phalloidin 488 and 4, 6-diamidine-2%-Phenylindole (DAPI) in BSA/PBS, the solution for staining cells was prepared. This solution was added to the samples and incubated for 30 min. Finally, the samples were washed 3 times with PBS/A and the cells were observed by fluorescent microscope (Olympus, Japan).

3.9. Statistical Analysis

Using GraphPad InStat software (USA) statistical differences were determined. All data were given with the mean ± standard deviation of three replicates. $p< 0.05$ values were accepted as significant. (Two-way Student's t-test and One-way ANOVA method were used to evaluate significant differences between groups).

4. RESULTS

4.1. Raw Wheat Starch Moisture Evaporation Percentage During Drying

Considering that the final weight of 10 g of raw starch, which was dried in two stages of 24 and 12 h at temperatures of 100°C and 60°C, respectively, which was 9.2 g, the moisture evaporation content of raw starch was measured from the formula mentioned in the methods parts. The result obtained from the mass reduction of crude starch showed that this amount was 8%. The aim of this test is drying can reduce gelatinization temperature [52].

4.2. SEM Analysis of the Raw and Dried Wheat Starch Granules

According to the literature, wheat starch granules have a lenticular shape with indentations and consist of small and large size types, with an average diameter of 4 and 14 µm respectively [11, 52]. SEM analysis was performed to evaluate the morphology, size, and shape of raw and dried wheat starch (See Figure 4.1 and Figure 4.2). The size of small and large raw wheat starch granules was measured as 19.43 ± 2.80 µm and 5.27 ±2 .37 µm, respectively. Dried granules, for small and large types, were measured as 20.17 ± 3.92 µm and 4.90 ± 1.35 µm, respectively. It is noteworthy that the surface of the raw granules is almost free of defects, but in the dried starch due to the drying process, the granules are damaged and their surfaces have more defects and scratches. The scratches presumably were to have been caused by the local explosive release of water vapor [52].

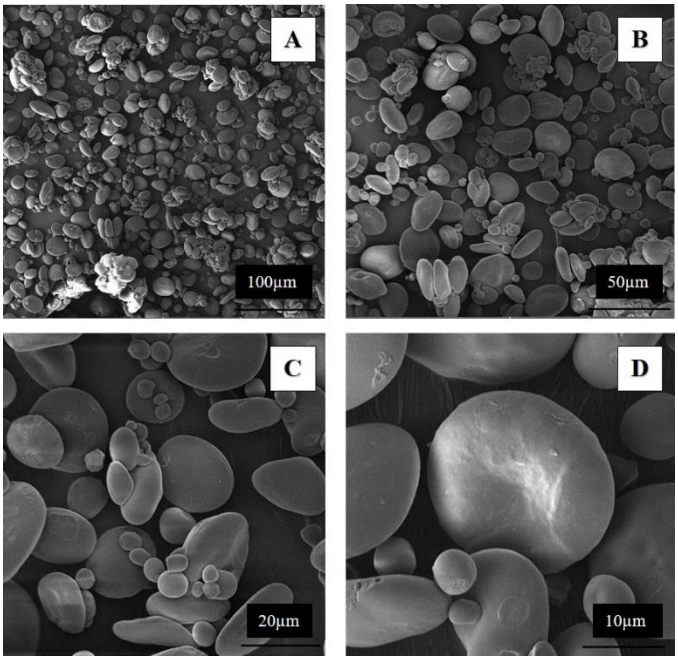

Figure 4.1. SEM microghraphs of raw wheat starch granules at A) 500X B) 1000X C) 2500 X D) 5000 magifications.

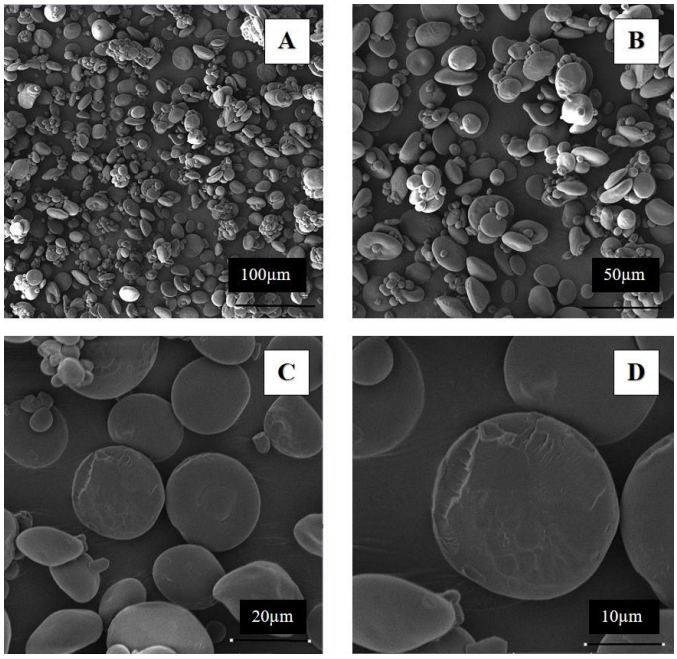

Figure 4.2. SEM microghraphs of dried wheat starch granules at A) 500X B) 1000X C) 2500 X D) 5000 magifications.

4.3. Gelatinization and Solubility of Starch Granules from Different Sources

During the hydration of starch by the water as the most common plasticizer, swelling of granules occurs. If the event simultaneously happened by heating starch to about 60-80°C (depending on the source of starch), irreversible swelling and melting of the crystalline

region in granules were occurs. The mentioned phenomenon is known as the gelatinization process [12]. It is noteworthy that when the temperature rises, the water first affects the amorphous regions of the granules, where the first swelling occurs, but this event causes forces to destroy the crystalline regions, and eventually, the polysaccharide which is soluble in the water obtained [26].

According to the microscope images of wheat starch granules, these granules begin to absorb water at a temperature of 25°C and have not yet reached their maximum absorption at a temperature of 55°C. But at a temperature of 85°C, the outer layers of the granules still maintain their structure, but it seems that the molecules inside the granules are dissolved in water (See Figure 4.3).

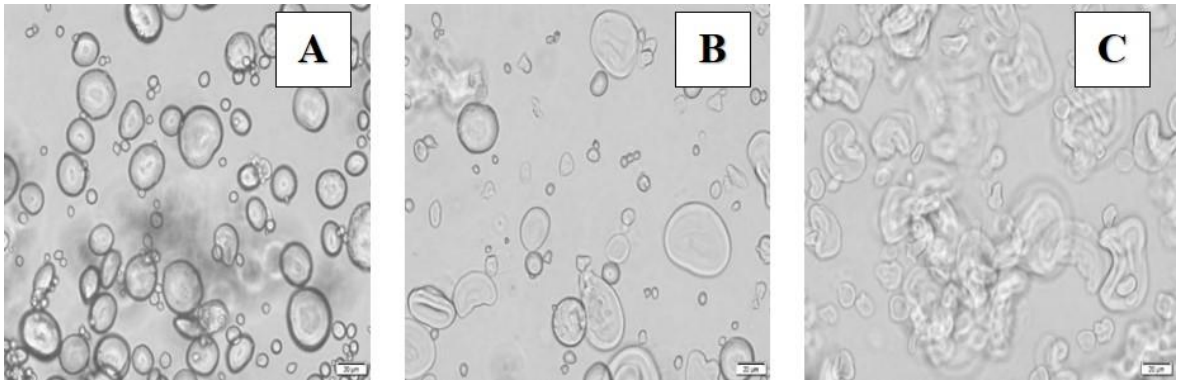

Figure 4.3. Microscope images of wheat starch granules in water at A) 25°C, B) 55°C and C) 85°C, respectively.

Corn starch granules are polyhedral in shape which is notable in microscope images [11]. In the investigation of corn starch granules in water under conditions of increased temperature Corn starch absorbed very little water at a temperature of 25°C. At a temperature of 55° C, the absorption of water has occurred on average, while at a temperature of 85°C, the absorption of water has nearly reached its maximum, and the outer layers of corn granules still maintain the overall structure of the granules (see Figure 4.4).

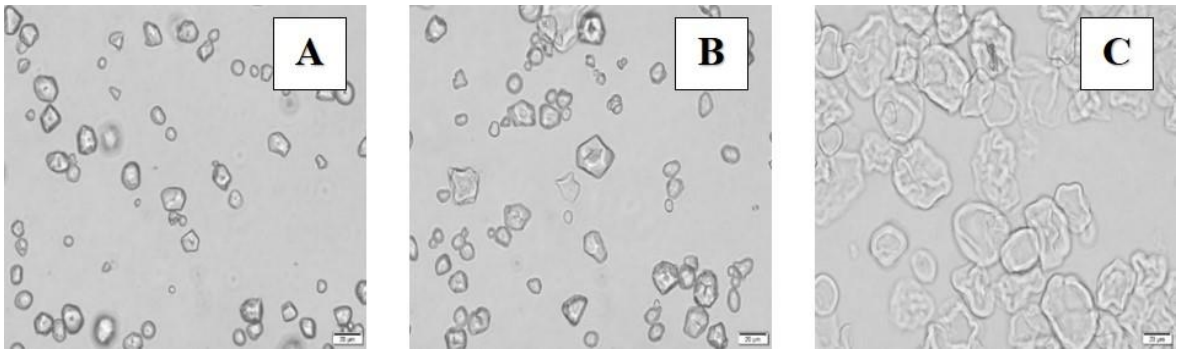

Figure 4.4. Microscope images of corn starch granules in water at A) 25°C, B) 55°C and C) 85°C, respectively.

In examining the behavior of rice starch granules, it should be said that these granules have strongly absorbed water at a temperature of 25°C compared to wheat and corn, and at a temperature of 55°C, the structure of these granules is going to destructure, and at a temperature of 85°C disintegration has occurred completely and a homogeneous solution is seen (see Figure 4.5).

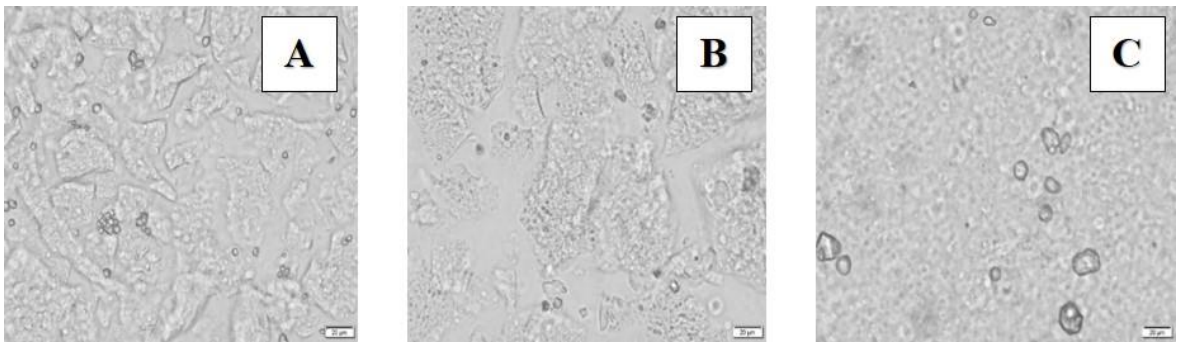

Figure 4.5. Microscope images of rice starch granules in water at A) 25°C, B) 55°C, and C) 85°C, respectively.

4.4. Film Characterization

4.4.1 TPS Films' Physical Appearance

Macroscopic appearances of all fabricated wheat TPS films indicated that films with total plasticizers of 30% and 40% had a stable physical condition in comparison with groups of films with total plasticizers of 50%, 60%, and 70%. It is notable that, in this study, an increase and reduction in the amount of glycerol compared to D-sorbitol in TPS films with the same total plasticizers ratio, respectively had led to an increment in stickiness and brittleness in their appearance. Due to the migration of the D-sorbitol and glycerol to the

surface of the films respectively brittleness and stickiness on the films are predictable and furthermore, during a period of time due to the retrogradation of the starches' molecules, migration of the plasticizers to the surface of the TPS films can promote [53, 54]. Half of the TPS films' groups because of the saccharification, higher brittleness, higher stickiness, and applying limitations in handling and effective use for further research were eliminated (See Table 4.1).

4.4.2. TPS Films' Thickness

All fabricated TPS films group present thicknesses in the range of 0.16 to 0.26 mm with low mean deviations which indicates successful uniformed fabrication of each group of films. Due to the results, generally, with increasing the amount of total plasticizer size of TPS films, increasing in the thickness of the films was observed (See Table 4.1). Plasticizers increase the volume of the films because they affect the intermolecular network structure of the polymer and restructure it, and therefore the thickness of the films increases [55]. To continue further analysis ten groups of the TPS films that showed a more stable appearance were selected.

4.4.3. Density of TPS Films

The results obtained from the measurement of the density values revealed that in groups with the same total plasticizer, the density of the films increases by an increment of the D-sorbitol content compared to the glycerol (See Table 4.1). It is noteworthy that D-sorbitol and glycerol used in this study have a density of 1.49 g/cm^3 and 1.26 g/cm^3, respectively. In another study sage seed gums, films were fabricated with sorbitol and glycerol separately, in the same ratio as a plasticizer. This study revealed that fabricated films with glycerol in comparison to the D-sorbitol presented lower density which is in agreement with the results of the current study [55, 56].

Table 4.1. Thermoplastic wheat starch films' composition, thickness, density, and physical appearance (Percentages of plasticizers are determined according to the starch total weight. S and G letters are representative of D-sorbitol and Glycerol respectively and numbers left to the letters indicate the ratio of each plasticizer to its total).

Total Plasticizer (%)	D-sorbitol (%)	Glycerol (%)	Film	Thickness (mm)	Density (g/cm^3)	Physical Appearance
30	10	20	10S-20G	0.17±0.01	1.22±0.12	Stable
	20	10	20S-10G	0.18±0.01	1.44±0.01	Stable
40	10	30	10S-30G	0.17±0.01	1.11±0.13	Stable
	20	20	20S-20G	0.16±0.03	1.16±0.27	Stable
	30	10	30S-10G	0.16±0.00	1.45±0.00	Brittle*
50	10	40	10S-40G	0.17±0.02	1.30±0.15	Stable
	20	30	20S-30G	0.23±0.04	1.13±0.27	Stable
	30	20	30S-20G	0.20±0.05	1.32±0.00	Brittle*
	40	10	40S-10G	0.17±0.01	1.56±0.00	Brittle*
60	10	50	10S-50G	0.25±0.04	0.97±0.13	Stable
	20	40	20S-40G	0.22±0.03	1.10±0.16	Stable
	30	30	30S-30G	0.21±0.02	1.00±0.01	Saccharification*
	40	20	40S-20G	0.20±0.01	1.32±0.12	Stable
	50	10	50S-10G	0.23±0.03	1.29±0.00	Saccharification*
70	10	60	10S-60G	0.25±0.02	0.95±0.00	Sticky*
	20	50	20S-50G	0.26±0.02	1.01±0.00	Sticky*
	30	40	30S-40G	0.25±0.02	1.05±0.00	Sticky*
	40	30	40S-30G	0.21±0.01	1.28±0.02	Stable
	50	20	50S-20G	0.19±0.02	1.37±0.00	Saccharification*
	60	10	60S-10G	0.21±0.01	1.45±0.00	Saccharification*

**Could not manipulated*

4.4.4. Moisture Content Analysis

The moisture content values of the TPS films indicated that in the groups with the same total plasticizer by reduction of the glycerol ratio to the D-sorbitol, the moisture contents of the films were reduced (See Table 4.2). Due to the high molecular similarity of sorbitol with

glucose units of the starch polymer, it is likely to establish a strong intermolecular bond in comparison with glycerol and starch chains. Glycerol has a premier affinity with water molecules in comparison with sorbitol which leads to superior moisture content values in TPS films containing a higher ratio of glycerol compared to sorbitol [55, 57].

4.4.5. Water Solubility Analysis

Water solubility percentage values of the fabricated TPS films indicated that an increase in the total amounts of the plasticizer, which varies from 30% to 70%, led to an increase in the values of this property. Furthermore, results presented that in the films with the same total plasticizers, by reduction of the D-sorbitol ratio to the glycerol, their water solubility property decreased (See Table 4.2). The ratio and type of plasticizers that utilizes in fabricating the TPS, influence their water solubility ability [58, 59]. Glycerol and D-sorbitol as hydrophilic plasticizers weaken the interaction of the starch chains together and create free volume in TPS, consequently, increasing the water diffusion amount to the TPS matrix, and the water solubility [55].

Table 4.2. Thermoplastic wheat starch films' composition, moisture content and water solubility (Percentages of plasticizers are determined according to the starch total weight. S and G letters are representative of D-sorbitol and Glycerol respectively and numbers left to the letters indicate the ratio of each plasticizer to its total).

Total Plasticizer (%)	D-Sorbitol (%)	Glycerol (%)	Film	Moisture Content (%)	Water Solubility (%)
30	10	20	10S-20G	1.89±3.00	21.84±2.49
	20	10	20S-10G	16.93±4.67	26.64±2.99
40	10	30	10S-30G	22.21±0.85	21.20±0.92
	20	20	20S-20G	17.77±1.84	25.78±1.88
	30	10	30S-10G	12.36±0.00	28.74±0.00
50	10	40	10S-40G	24.87±2.60	22.22±0.58
	20	30	20S-30G	18.10±6.86	27.54±1.47
	30	20	30S-20G	19.23±0.00	29.58±0.00
	40	10	40S-10G	12.51±0.00	34.50±0.00
60	10	50	10S-50G	34.85±1.50	22.45±1.73
	20	40	20S-40G	24.54±1.28	28.19±4.30
	30	30	30S-30G	20.34±0.00	31.86±0.00
	40	20	40S-20G	19.08±2.27	30.81±0.52
	50	10	50S-10G	13.45±0.00	49.32±0.00
70	10	60	10S-60G	30.21±0.00	23.32±0.00
	20	50	20S-50G	34.23±0.00	32.38±0.00
	30	40	30S-40G	19.40±0.00	34.67±0.00
	40	30	40S-30G	22.10±3.81	35.31±1.56
	50	20	50S-20G	10.68±0.00	36.47±0.00
	60	10	60S-10G	8.41±0.00	43.61±0.00

4.4.6. Mechanical Test

In the current study, tensile strength and elastic modulus measurement indicated that the TPS films with total plasticizer ratios of 30% and 40% had a better performance in comparison with the other ten groups. TPS film with 40% total plasticizer and an equal ratio of glycerol and D-sorbitol presented the highest tensile strength and a Young modulus with values of 11.35 MPa and 576.55 MPa respectively. Conversely, results obtained from the breaking strain test were shown that mostly TPS films in high total plasticizers have better performance, however, the TPS film with 30% total plasticizer and the D-sorbitol to glycerol ratio of 2, presented considerable performance too, and in the toughness analysis submitted the highest value of the 2.05 MPa. The TPS film with 60% total plasticizer and the D-sorbitol to glycerol ratio of 2/4, with a high breaking strain of about 66.12% submitted the best performance. The direct relationship between the percentage of the plasticizers and the toughness value could not be detected. Many studies have shown that increases in the plasticizer ratio led to a reduction in the tensile strength values [60, 61]. The reason for using plasticizers is to weaken the interaction of starch molecular chains and to form hydrogen bonds with starch chains, consequently flexibility of the TPS films increase [62]. According to the results obtained from the analysis up to this stage, 6 groups of films were selected for the next analysis due to their pioneer properties. (See Figure 4.6 & Table 4.3)

Table 4.3. Mechanical tests values of TPS films with total plasticizer: 30% (10S-20G), 30% (20S-10G), 40% (10S-30G), 40% (20S-20G), 50% (10S-40G), 50% (20S-30G), 60% (10S-50G), 60% (20S-40G), 60% (40S-20G), 70% (40S-30G).

Film	Tensile Strength (MPa)	Breaking Strain (%)	Toughness (MPa)	Elastic Modulus (MPa)
10S-20G	9.02 ± 1.29	15.06 ± 3.98	0.85 ± 0.38	382.20 ± 28.00
20S-10G	3.99 ± 0.46	66.05 ± 16.09	2.05 ± 0.59	76.50 ± 16.92
10S-30G	6.78 ± 1.33	27.15 ± 13.13	1.37 ± 0.49	122.45 ± 5.73
20S-20G	11.35 ± 7.65	13.08 ± 9.48	0.82 ± 0.17	576.55 ± 12.80
10S-40G	4.05 ± 0.40	25.94 ± 6.69	0.76 ± 0.23	117.15 ± 9.40
20S-30G	3.72 ± 0.41	38.17 ± 5.47	1.16 ± 0.00	87.05 ± 24.40
10S-50G	0.53 ± 0.11	32.72 ± 4.70	0.11 ± 0.03	3.87 ± 1.45
20S-40G	2.24 ± 0.05	66.12 ± 3.17	1.11 ± 0.06	23.55 ± 0.64
40S-20G	1.74 ± 0.23	31.48 ± 8.83	0.38 ± 0.14	18.69 ± 3.71
40S-30G	0.82 ± 0.16	64.69 ± 5.51	0.29 ± 0.09	2.00 ± 0.29

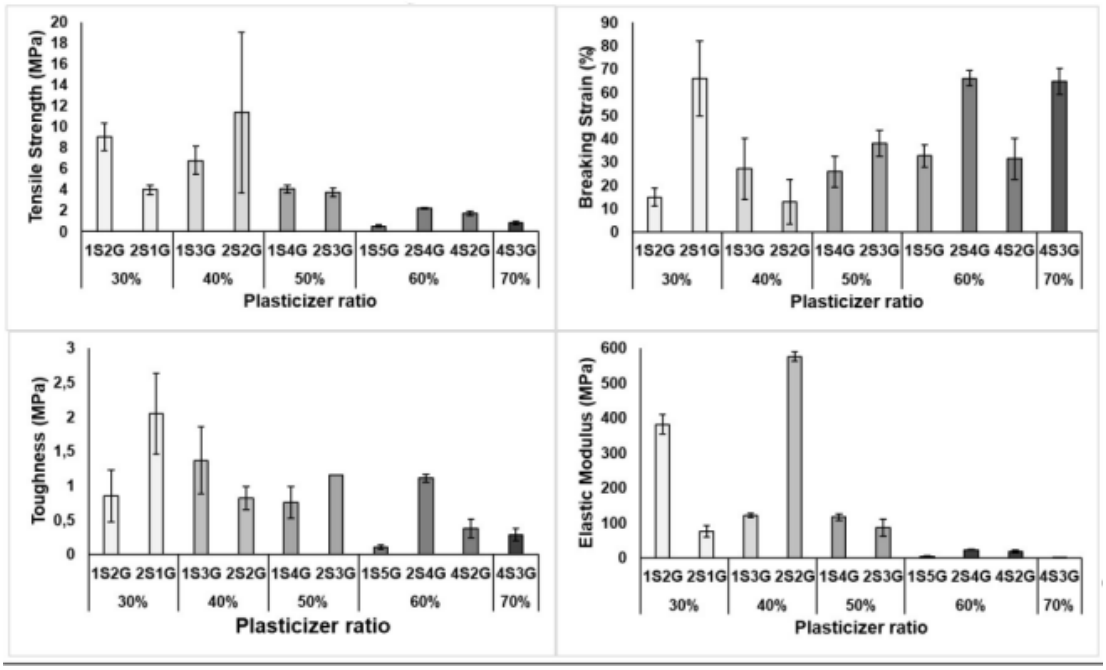

Figure 4.6. Plasticizer effects on tensile strength, breaking strain, toughness, and elastic modulus properties of TPS films with total plasticizer: 30% (10S-20G), 30% (20S-10G), 40% (10S-30G), 40% (20S-20G), 50% (10S-40G), 50% (20S-30G), 60% (10S-50G), 60% (20S-40G), 60% (40S-20G), 70% (40S-30G).

4.4.7. Attenuated Total Reflectance-Fourier Transform Infrared (ATR- FTIR) Analysis

IR spectra of the raw and dried starch, D-sorbitol, glycerol, and 6 selected groups of the TPS films are presented in Figure 4.7. Due to the interaction of the O-H groups in plasticizers and starch chains, absorption in 3600−3020 cm^{-1} wavelength ranges, which belong to the hydrogen bond, have seen [55, 63]. In the comparison of the dried starch with raw starch spectra in this wavelength, the wave magnitude reduced, which indicates a reduction in starch moisture. Absorption peaks around 2950 cm^{-1} and 1680 cm^{-1} wavelengths, respectively ascribed to C-H aliphatic and water molecular bonds in starch [55]. In D-sorbitol and glycerol IR spectra in 1500 to 1200 cm^{-1} wavelength ranges, peaks which ascribe O-H bending and overlapping of C-H and due to stretching of COH, in 2917 cm^{-1} wavelength absorption peaks were seen [64]. In detail about the glycerol IR spectra, should be mentioned that peaks about 1145 and 962 cm^{-1} ascribe C-O stretching [65]. About D-sorbitol spectra, it is notable that maximum absorption in 1046 and 1084 cm^{-1} wavelengths are responsible for vibration of C-OH and in 1411 and 890 cm^{-1} ascribe O-H bending vibration [66]. Polysaccharides have their own distinctive peaks which appeared in 800 to 1200 cm^{-1}

wavelengths Stretching vibration of the attached C-O and C-C is responsible for characteristics peaks of the starch, which appear in 1150, 1010, and 1080 cm^{-1} wavelengths [67]. In fabricated TPS films, which were prepared with starch, glycerol and D-sorbitol IR spectra's wide band appeared in 3000 to 3700 cm^{-1} wavelengths, which is due to the O-H stretching related to the hydroxyl groups, and in 3000 to 2800 cm^{-1} wavelengths regions peaks are associated with C-H stretching [58]. (See Table 4.4)

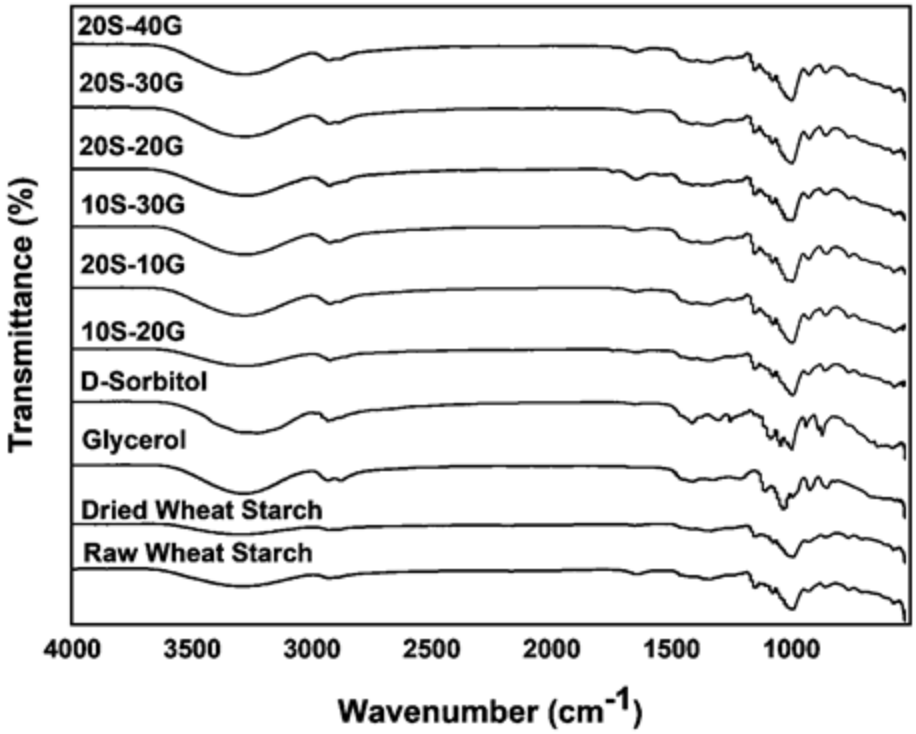

Figure 4.7. FTIR spectra of raw wheat starch, dried wheat starch, glycerol, D-sorbitol and the six selected TPS films with total plasticizer: (B) 30% (10S-20G), (C) 30% (20S-10G), (D) 40% (20S-20G), (E) 40% (10S-30G), (F) 50% (20S-30G), (G) 60% (20S-40G).

Table 4.4. FTIR characteristic peaks wavenumber of raw wheat starch, dried wheat starch, glycerol, D-sorbitol and the six selected TPS films with total plasticizer: (B) 30% (10S- 20G), (C) 30% (20S-10G), (D) 40% (20S-20G), (E) 40% (10S-30G), (F) 50% (20S-30G), (G) 60% (20S-40G).

Sample	Wavenumber (cm^{-1})	Peak Characteristics
Glycerol	2917	symmetrical stretching of COH
	1145 and 962	C-O stretching
D-sorbitol	890 and 1411	O-H bending
	1046 and 1084	C-OH stretching
Glycerol and D-sorbitol	3300	O - H stretching
	2800-3000	C - H stretching
	1500-1200	overlapping of C-H in planes O-H bending
Wheat starch	800-1200	characteristic peaks of polysaccharides
	1010, 1080 and 1150	C-O and C-C stretching

4.4.8. Hydrolytic Degradation Tests

The hydrolytic degradation property of the materials is one of the important factors in biomedical research. The fragile bonds of the polymer chains can create bonds with water which leads them to break into small chains, in this case, the hydrolysis mechanism causes degradation [44]. In this test, for simulating human body conditions, to reach the closely real degradation rate of the TPS films, they were suspended in PBS buffer at 37°C with a shaking rate of 50 rpm condition. The obtained results revealed that in the groups of the films with equal total plasticizer, increasing the D-sorbitol to the glycerol ratio, mass loss of the TPS decreased, which presented lower hydrolytic degradation. This may be due to the fact that D-sorbitol binds more strongly to starch in comparison with glycerol, which increases the water-resistance property of the TPSs, and it is notable, glycerol has more affinity with water [55, 57]. The results also presented that the group with 60% total plasticizer in this test, had the highest weight loss with a 49% value. Conversely, TPS film groups with total plasticizer of 30% and 40% respectively, with D-sorbitol to glycerol ratios of 2/1 and 2/2 presented the lowest mass loss percentage at about 39 with the lowest degradation rate. (See Figure 4.8)

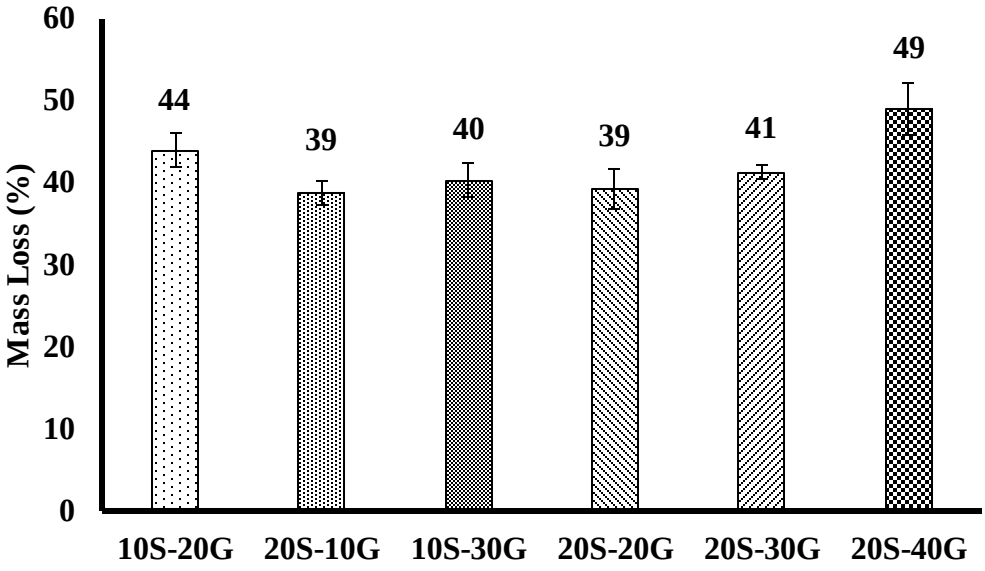

Figure 4.8. Hydrolytic degradation behaviors, of the six selected TPS films with total plasticizer: 30% (10S-20G), 30% (20S-10G), 40% (10S-30G), 40% (20S-20G), 50% (20S- 30G), 60% (20S-40G).

4.4.9. Determining Water Uptake Capacities

Thermoplastic starch films have hydrophilic properties. To investigate the effect of type and amount of plasticizers on the ratio of water absorption and swelling of the films, they were immersed in PBS, which simulate body fluids, at 37°C condition. The number of hydroxyl groups in the film structure is limited, so as can be seen from the resulting graph of this test, the rate of water absorption is higher in the early times so swelling occurs, and over time this rate decreases and reaches equilibrium [55]. The approximate constant rate of water absorption at the last moment of this test is due to the fact that the hydroxyl active groups are saturated [55]. The resulting graph presented that groups with 60% and 50% plasticizers have the lowest water absorption and swelling rate, which can be related to the effect of the ratio of plasticizers on the water resistance of the films. D-sorbitol in comparison with glycerol has a strong bond with starch chains and as mentioned glycerol affinity with water is higher than sorbitol. In groups with equal total plasticizers, by increasing the amount of D-sorbitol to glycerol, the water absorption and swelling rate of the films were reduced. The results obtained from tests revealed that an increase in the total amount of the plasticizers led to a decrease in water absorption and swelling of the TPS films (See Figure 4.9). Other studies also support these results [55, 68].

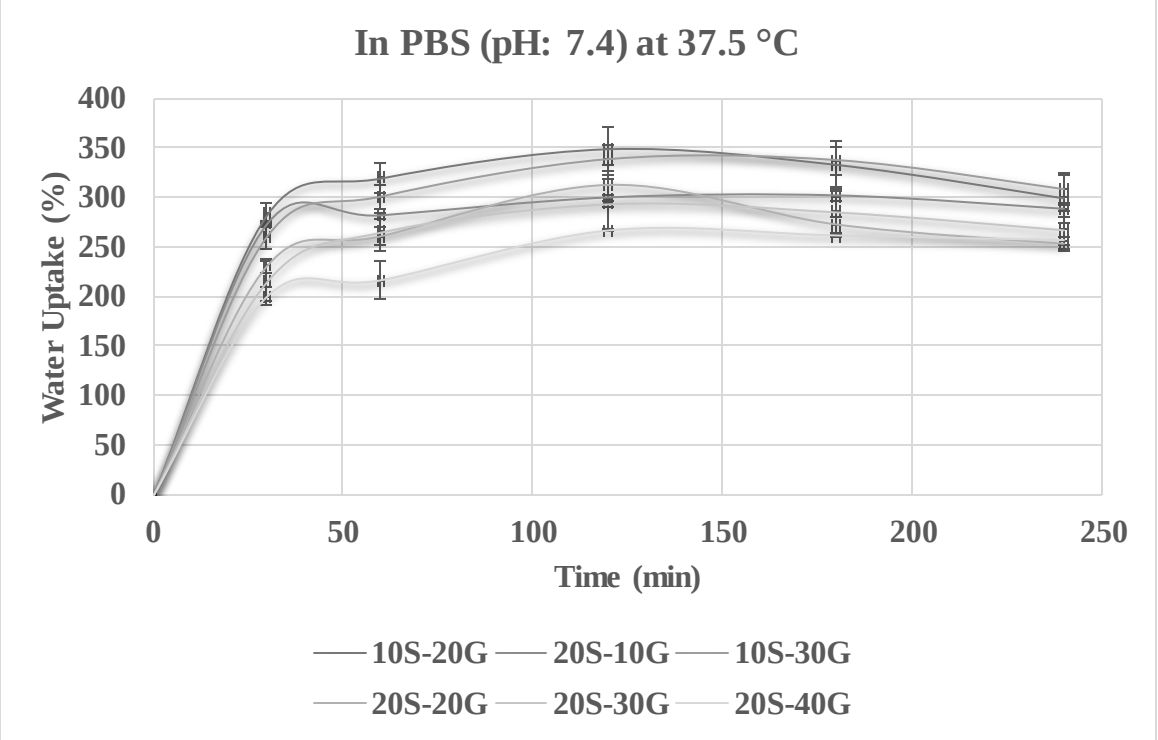

Figure 4.9. Water uptake capacities, of the six selected TPS films with total plasticizer: 30% (10S-20G), 30% (20S-10G), 40% (10S-30G), 40% (20S-20G), 50% (20S-30G), 60% (20S- 40G).

4.4.10. X-Ray Diffraction (XRD) Analysis

The peaks of the XRD patterns, which indicate the crystallinity of the films and the wheat starch, show that the films have less crystallinity than the starch, which is due to the reaction of the plasticizers with the starch chains that leads to the destruction of the starch crystalline network. Furthermore, the results from XRD patterns revealed that groups with 40% and 50% total plasticizers with a D-sorbitol to glycerol ratio of 2/2 and 3/2 respectively, have a lower percentage of crystallinity and a larger amorphous area. In the XRD pattern of wheat starch, peaks at 2θ were seen with values of the 11.3°, 15.2°, 17.3°, 18.1°, 23.3°, and 26.7° which represented A-crystallinity type in starch structure (See Figure 4.10) [69].

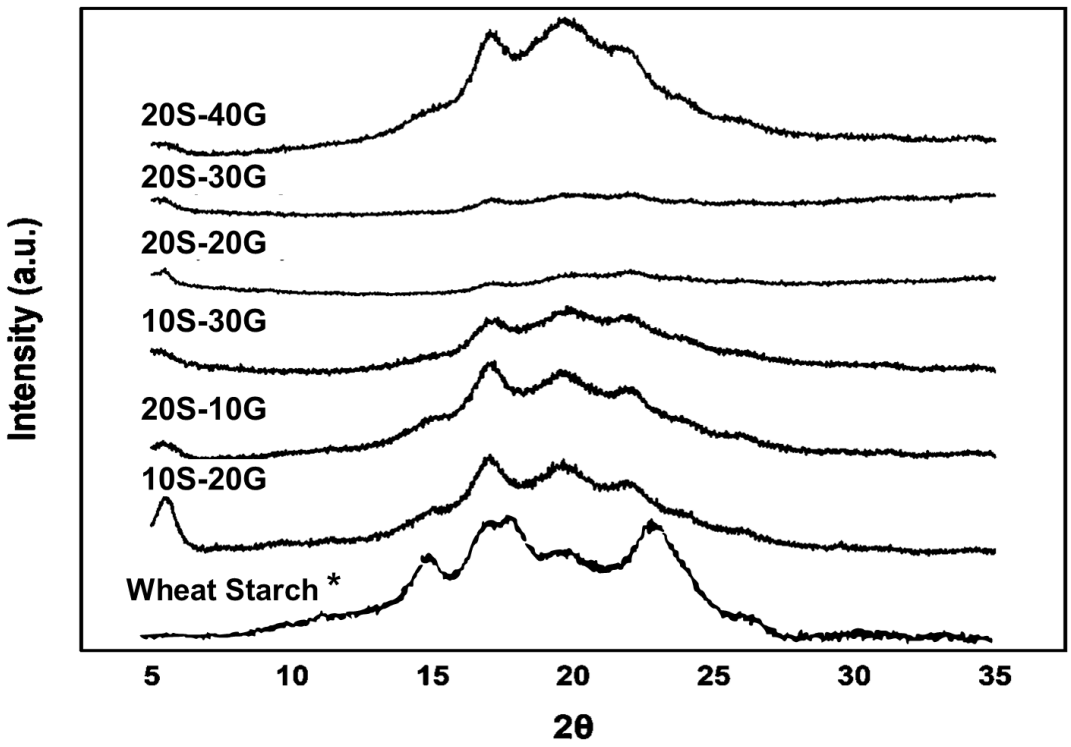

Figure 4.10. XRD patterns of 30% (10S-20G), 30% (20S-10G), 40% (10S-30G), 40% (20S-20G), 50% (20S-30G), 60% (20S-40G). (*Wheat starch XRD pattern adapted from [69]).

Table 4.5. Crystallinity percentages of six selected film.

Sample	Crystallinity %
10S-20G	32.9
20S-10G	31.7
10S-30G	30.7
20S-20G	21.5
20S-30G	24.7
20S-40G	39.2

4.4.11. Water Contact Angle (WCA) Measurements

Starch thermoplastic films have hydrophilic properties [70]. Water contact measurement analysis was performed to measure fabricated TPS films' water wettability abilities. The water contact structure on the thermoplastic composite surface shows the interactions of the hydrogen bonds of the water with the surface of the TPS [71]. The hydrophobic properties of a material increase the contact angle of water with it compared to hydrophilic material

[72]. The results of this test revealed that the group with 60% total plasticizer had the highest hydrophilicity, which is probably due to the high glycerol content, which is more hydrophilic than sorbitol. Also, according to the results of SEM analysis, it can be due to the migration of plasticizers to the surface of the films. The group with a 30% total plasticizer with a D-sorbitol to glycerol ratio of 2 had more hydrophobic properties than the other groups. The rest of the groups approximately presented hydrophilic properties. (Table 4.6) Furthermore, it is considerable, that the wettability of the biomaterial surface plays a crucial role in the early stage of cell adhesion [73].

Table 4.6. Wettability properties of the six selected TPS films with total plasticizer: 30% (10S-20G), 30% (20S-10G), 40% (10S-30G), 40% (20S-20G), 50% (20S-30G), 60% (20S-40G).

Sample	Water Contact Angle (°)
10S-20G	91.1 ± 0.8
20S-10G	113.9 ± 1.3
10S-30G	87.0 ± 0.7
20S-20G	81.6 ± 0.6
20S-30G	89.9 ± 1.7
20S-40G	58.4 ± 0.8

4.4.12. Film Roughness Analysis

Roughness analysis of the films' surfaces was performed using a perthometer, the results obtained from the tests revealed that in groups with the same total plasticizer increasing in the D-sorbitol ratio caused a decrease in roughness and almost the results obtained from the measurement of roughness support the results obtained from SEM analysis. (Table 4.7)

Table 4.7. Roughness properties of the six selected TPS films with total plasticizer: 30% (10S-20G), 30% (20S-10G), 40% (10S-30G), 40% (20S-20G), 50% (20S-30G), 60% (20S- 40G).

Sample	Roughness, Ra (µm)
10S-20G	0.53 ± 0.07
20S-10G	0.41 ± 0.10
10S-30G	0.53 ± 0.10
20S-20G	0.48 ± 0.08
20S-30G	0.33 ± 0.02
20S-40G	0.62 ± 0.12

4.4.13. Thermogravimetric Analysis (TGA)

Generally, TPS films' TGA curves presented three thermal degradation phases. Evaporation of plasticizers, molecules with low weight, and free water led to the creation of the first stage and in the second stage, some plasticizers decomposed and the starch is in the rich phase, and in the last stage starch oxidized, which before was in a partially decomposed condition [74,75]. TPS films in the first phase showed more stability in temperature-rising conditions and in comparison to the starch, loosed lower mass, and furthermore, in the groups with the same total plasticizer ratio, increasing the amount of D-sorbitol compared to glycerol caused more temperature stability in the TPS films. This can be due to lower volatility and a strong bond of the sorbitol with starch in comparison with glycerol [54]. (See Table 4.8 and Figure 4.11). Other research has shown that in starch thermoplastic films fabricated with glycerol, D-sorbitol, and both of them, glycerol-plasticized films presented lower thermal stability because glycerol bonds weaker with starch molecules than sorbitol [54] and sorbitol plasticized TPS films presented higher decomposition temperature [54].

Table 4.8. TGA data of (A) raw wheat starch, (B) dried wheat starch and the TPS films with total plasticizer: (C) 30% (10S-20G), (D) 30% (20S,-10G), (E) 40% (10S-30G), (F) 40% (20S-20G), (G) 50% (20S-30G), (H) 60% (20S-40G).

TGA							
	Sample	Onset Temp.[1] (°C)	Mass Loss I (%)	Onset Temp.[2] (°C)	Mass Loss II (%)	Onset Temp.[3] (°C)	Mass Loss III (%)
A	Raw Wheat Starch	51.9	9.3	-	-	305.8	71.8
B	Dried Wheat Starch	68.7	8.1	307.8	82.2	392.6	4.5
C	10S-20G	93.3	2.7	-	-	312.9	65.9
D	20S-10G	101.6	4.6	-	-	310.5	83.5
E	10S-30G	98.2	2.2	-	-	314.5	64.2
F	20S-20G	102.1	2.4	-	-	313.5	67.6
G	20S-30G	104.3	2.7	312.2	62.3	401.0	0.8
H	20S-40G	85.4	3.7	206.6	21.7	314.8	64.7

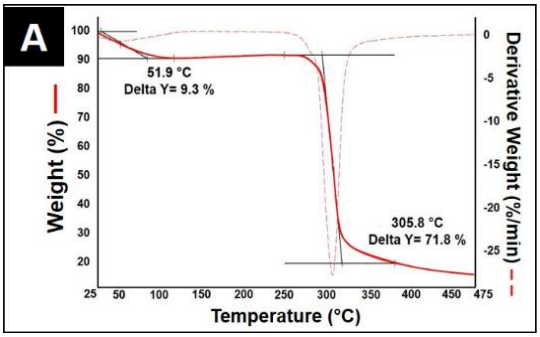

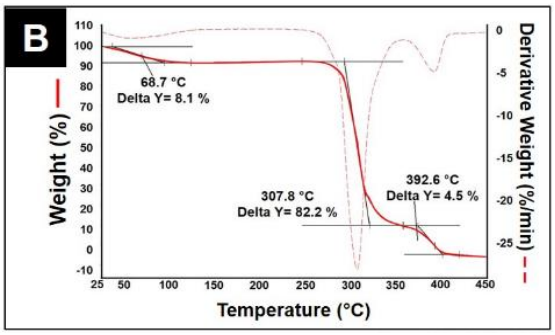

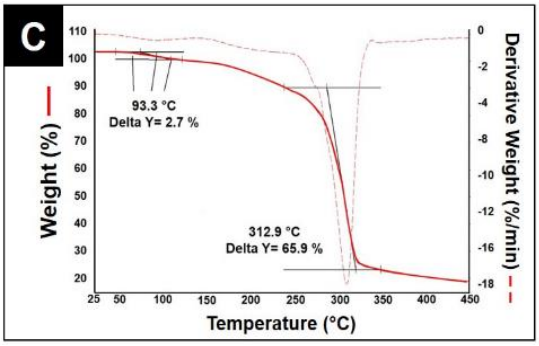

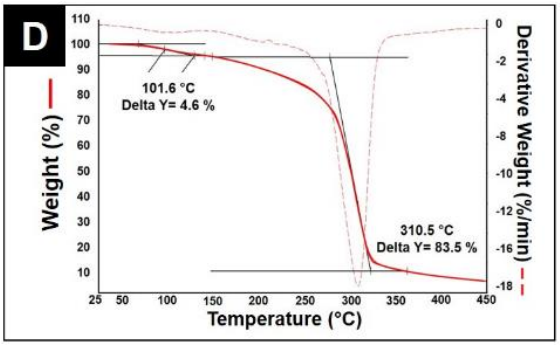

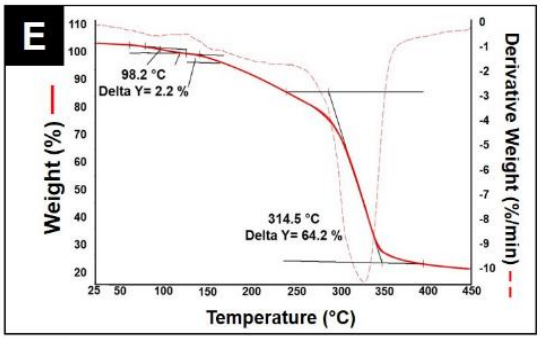

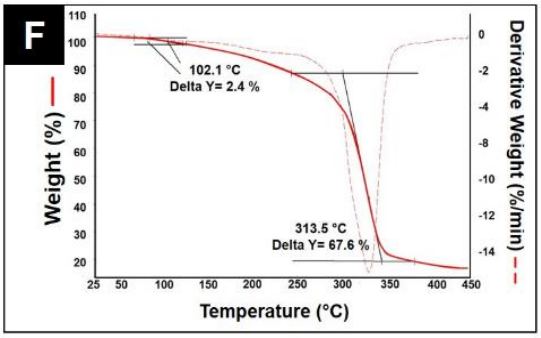

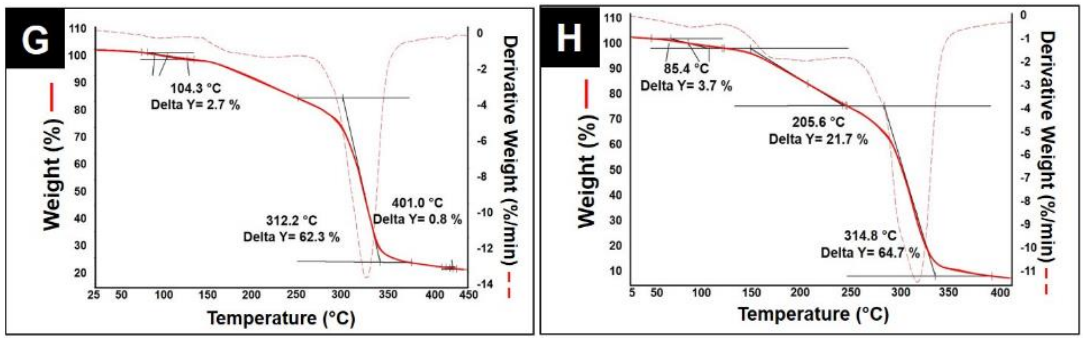

Figure 4.11. TGA graphs and of (A) raw wheat starch, (B) dried wheat starch and the TPS films with total plasticizer: (C) 30% (10S-20G), (D) 30% (20S-10G), (E) 40% (10S-30G), (F) 40% (20S-20G), (G) 50% (20S-30G), (H) 60% (20S-40G).

4.4.14. Differential Scanning Calorimetry (DSC) Analysis

In the endothermic diagram of the DSC of the native wheat starch, three peaks were observed, the first peak was related to the gelatinization temperature of the starch, the second peak was related to the melting temperature of amylose and fat complex and the third one was indicated decomposition temperature of the starch which is about 63.9°C, 112.3°C and 270.9°C for raw starch respectively [76-78]. The data obtained from the DSC results show that TPS films have higher decomposition temperatures due to the presence of plasticizers and an increment in the amount of plasticizer increases the decomposition temperature of the films (See Table 4.9). Films with plasticizers of 40%, 50%, and 60% presented a melting point, which indicates a decrease in the melting temperature of starch to below its decomposition temperature.

Table 4.9. DSC data of (A) raw wheat starch, (B) dried wheat starch and the TPS films with total plasticizer: (C) 30% (10S-20G), (D) 30% (20S-10G), (E) 40% (10S-30G), (F) 40% (20S-20G), (G) 50% (20S-30G), (H) 60% (20S-40G).

	T_P (°C)	T_M of fat/amylose complex (°C)	T_M (°C)	T_D (°C)
Raw Wheat Starch	63.9	112.3	-	220.8-270.9
Dried Wheat Starch	-	107.4	-	261.1
30% (1S2G)	-	-	-	291.3
30% (2S1G)	-	-	-	289.5
40% (1S3G)	-	-	168.6	319.4
40% (2S2G)	-	-	156.6	326.6
50% (2S3G)	-	-	177.6	308.3
60% (2S4G)	-	-	155.9	342.1

4.4.15. Scanning Electron Microscopy (SEM) Analysis

SEM analysis was performed to investigate the surface of the TPS films. This analysis provides useful information about the level of homogeneity and smoothness of the surfaces as well as the presence of fractures and cracks, which are important factors for selecting the proper material for industrial and biomedical applications [68]. In cellular studies, cells prefer rough surfaces on a nano scale to smooth ones, which can be an effective point in selecting fabricated films as the biomimetic membrane for cell growth for further studies [79]. SEM micrographs of the film surfaces presented that both groups of the TPS films with a total plasticizer of 30%, and the group with 40% plasticizer in an equal amount of D-sorbitol and glycerol have smooth, uniform, dense, and almost non-defects features. Films with 40% total plasticizer and a D-sorbitol to glycerol ratio of 1/3 presented very low roughness features. However, two groups with total plasticizers of 50% and 60% respectively presented very rough and cracky surfaces, which can presumably be due to the migration of the plasticizers to the surface of the films. In a detailed investigation, it is notable that increasing the ratio of the glycerol to the D-sorbitol leads to more defects and roughness in the film's surface, which is more visible in higher concentrations of total plasticizer (See Figure 4.12).

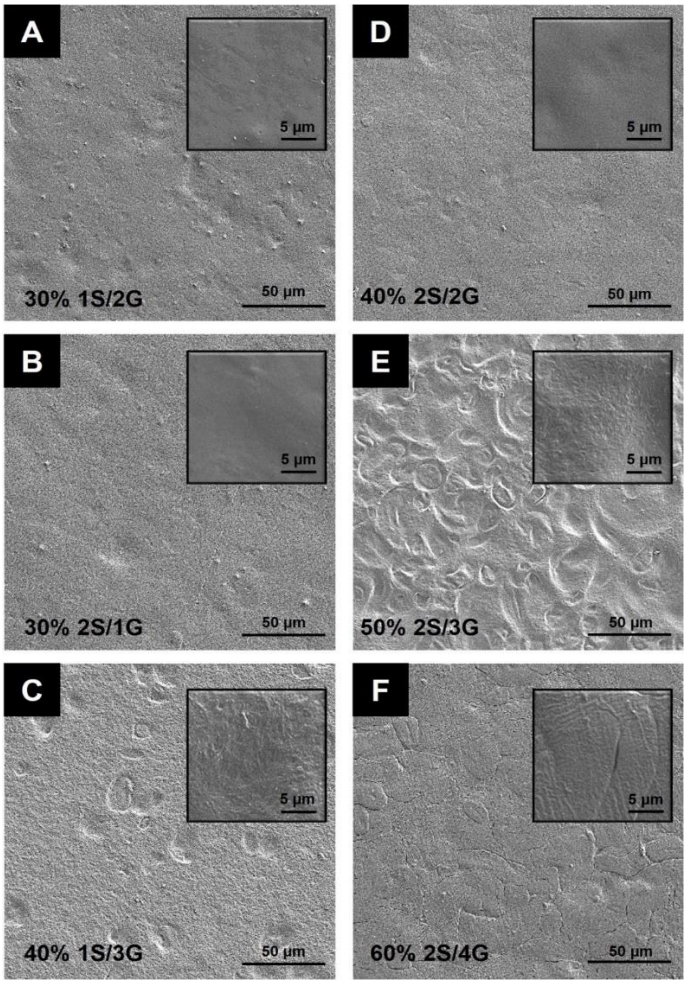

Figure 4.12. SEM images of the six selected TPS films with total plasticizer: (A) 30% (10S-20G), (B) 30% (20S-10G), (C) 40% (10S-30G), (D) 40% (20S-20G), (E) 50% (20S-30G), (F) 60% (20S-40G), at 1000X and 10000X magnifications, respectively.

4.5 Properties of TPS Solutions

4.5.1. Wheat TPS Solutions' Viscosity

The behavior of the TPS solution can be one of its most important features for analyzing its suitability for use in 3D bioprinting and other methods of experiments. In the results obtained from the results of viscosity, it should be said that solutions with 30% (10S-20G) and 60% (20S-40G) plasticizer showed the highest and lowest viscosity respectively, at temperatures of 15°C, 25°C, 37°C and 45°C. But at the temperature of 4°C, the solution with 40% (10S-30G) and 40% (20S-20G) showed the highest and lowest viscosity, respectively (Table 4.10). Amylose and amylopectin are responsible for gelling and viscosity of starch in water, respectively [27].

Table 4.10. Viscosity data of water and TPS solutions with total plasticizer 30% (10S-20G), 30% (20S-10G), 40% (10S-30G), 40% (20S-20G), 50% (20S-30G), 60% (20S-40G).

Temperature / Solution type	4°C	15°C	25°C	37°C	45°C
water	1.56	1.13	0.89	0.69	0.59
30% (10S-20G)	2.84	**2.02**	**1.56**	**1.13**	**0.93**
30% (20S-10G)	2.53	1.8	1.41	0.95	0.81
40% (10S-30G)	**2.91**	1.85	1.44	1.02	0.86
40% (20S-20G)	**2.51**	1.82	1.44	1.07	0.9
50% (20S-30G)	2.77	1.91	1.51	1.06	0.90
60% (20S-40G)	2.78	**1.62**	**1.26**	**0.88**	**0.76**

4.5.2. Wheat TPS Solutions' pH

pH is one of the most important influencing factors in tissue engineering experiments because cells must grow at a suitable pH that simulates human body fluids, at 37°C condition [55]. The pH of body fluids is 7.4 and the results obtained from measuring the pH of the TPS solution show that it can have suitable conditions for the growth of cells [55].

Table 4.11. pH of TPS solutions with total plasticizer 30% (10S-20G), 30% (20S-10G), 40% (10S-30G), 40% (20S-20G), 50% (20S-30G), 60% (20S-40G).

TPS solution type	pH
30% 10S-20G	7.45 ± 0.21
30% 20S-10G	7.56 ± 0.35
40% 10S-30G	7.54 ± 0.04
40% 20S-20G	7.74 ± 0.27
50% 20S-30G	7.48 ± 0.03
60% 20S-40G	7.49 ± 0.14

4.6. Characterization of Normal Human Dermal Fibroblast Cells

For cell culture studies Normal human dermal fibroblast (n-HDF) primary cells were supplied from Hacettepe University Center for Stem Cell Research and Development (PEDI-STEM). The characterization of these cells is very important to understand the behavior of these cells in further experiments. For this reason, characterization of n-HDF cells was performed with MTT analysis and cell count during 1^{st}, 2^{nd}, 3^{rd}, 5^{th}, 7^{th}, 10^{th}, and 14^{th} day of culturing. Morphology analysis of these cells was conducted by crystal violet staining on the 1^{st}, 3^{rd}, and 7^{th} days of the culture and, f-actin/DAPI staining on 3^{rd} day of culture.

4.6.1. Cell Count and MTT Analysis

According to the graph obtained from the results of cell counting (See Figure 4.13) lag phase, log phase, stationary phase, and death phase are observed in the growth curve. The cells entered the logarithmic phase on the 1^{st} day and they entered the death phase on the 10^{th} day. In order to obtain the cell growth curve 24, 48, and 72 hours, which are the closest time intervals to linearity, were selected from the graph and the natural logarithm (ln) of the number of cells at these hours was taken, and has been plotted against time. It was determined that the growth rate (μ) from the slope of the graph was 0.022 h^{-1}. In order to determine the cell doubling time, ln2 was divided by the growth rate using the formula $\ln2/\mu$ and the doubling time was determined to be 31.5 hours (See Figure 4.14).

$$t_d = \ln(2) / \mu \quad (7)$$

In Equation 7, μ and t_d respectively indicates specific growth rate and doubling time.

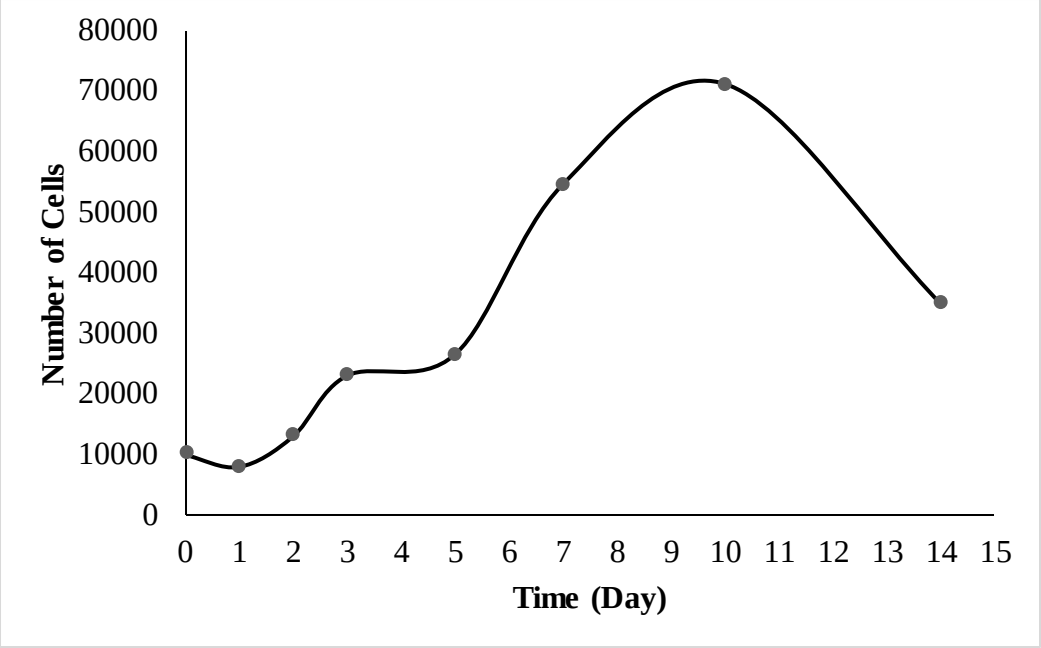

Figure 4.13. Cell count graph of n-HDF.

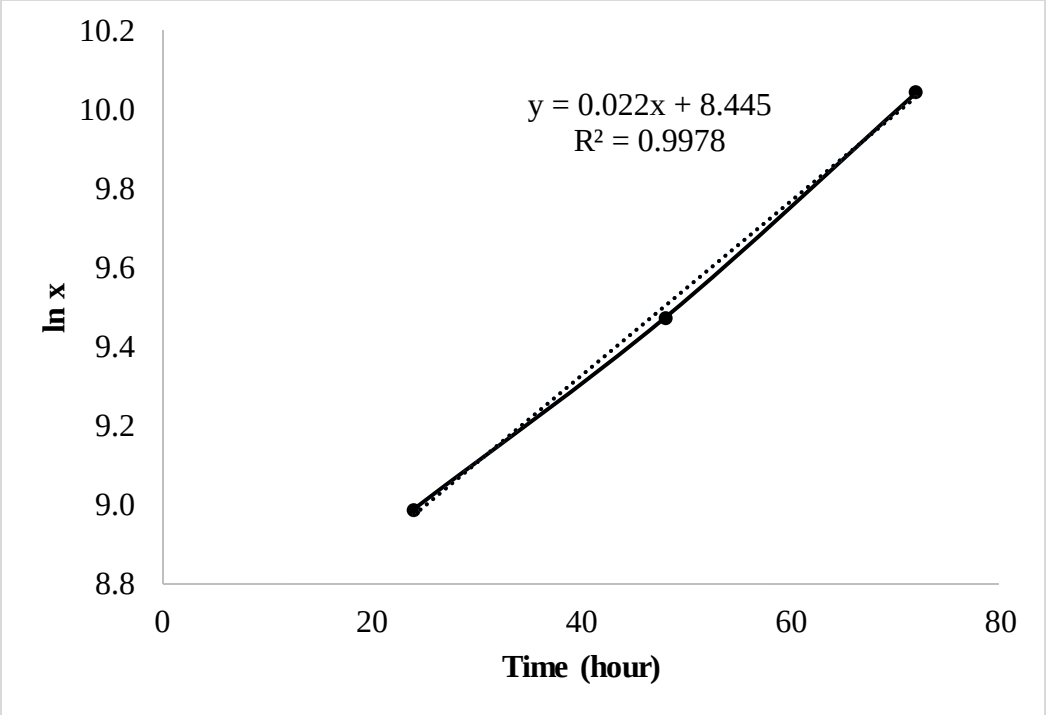

Figure 4.14. Growth curve of n-HDF cells.

Absorbance values were obtained on the specified days during the 14-day culture of n-HDF cells presented in Figure 4.15. The number of cells in the culture and the MTT analysis results were graphed together by considering the linear area in the cell growth curve, and the

absorbance values of the n-HDF cells as a result of the MTT analysis depending on the cell number were determined.

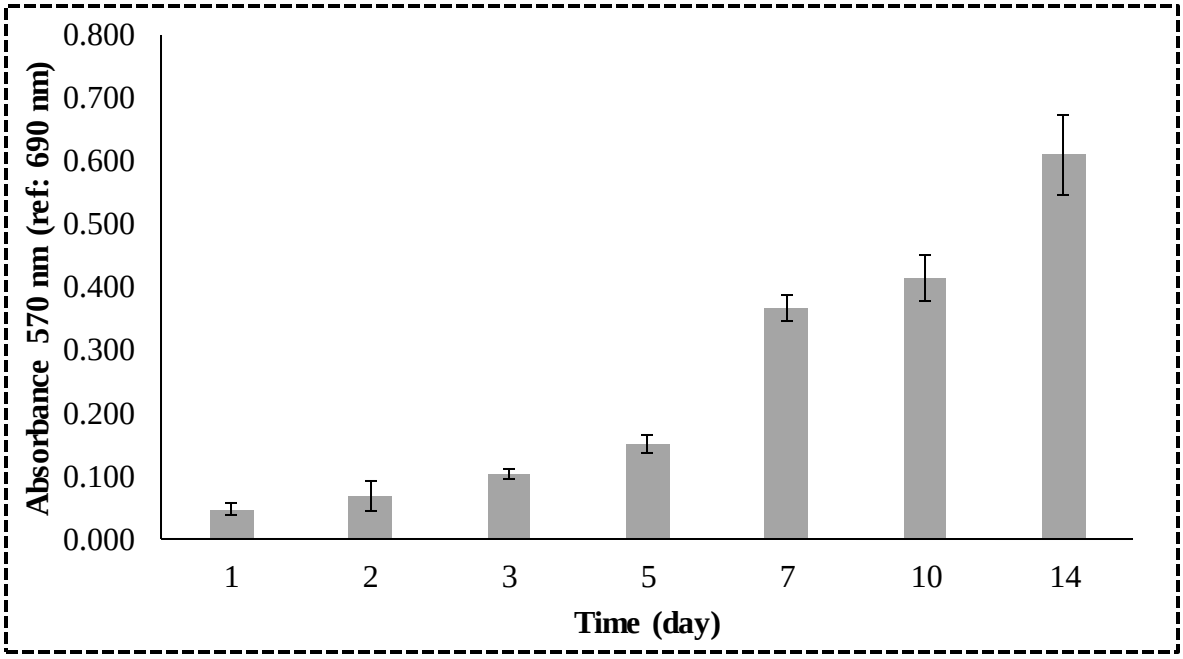

Figure 4.15. Absorbance values obtained on the specified days during the 14-day culture of N-HDF cells.

MTT results obtained at 24, 48 and 72 hours of culture showed an almost linear trend, based on the number of cells at 24, 48, and 72 hours of culture. From here, it was determined that the results obtained by the viability analysis and the results obtained as a result of the counting were in agreement (See Figure 4.16).

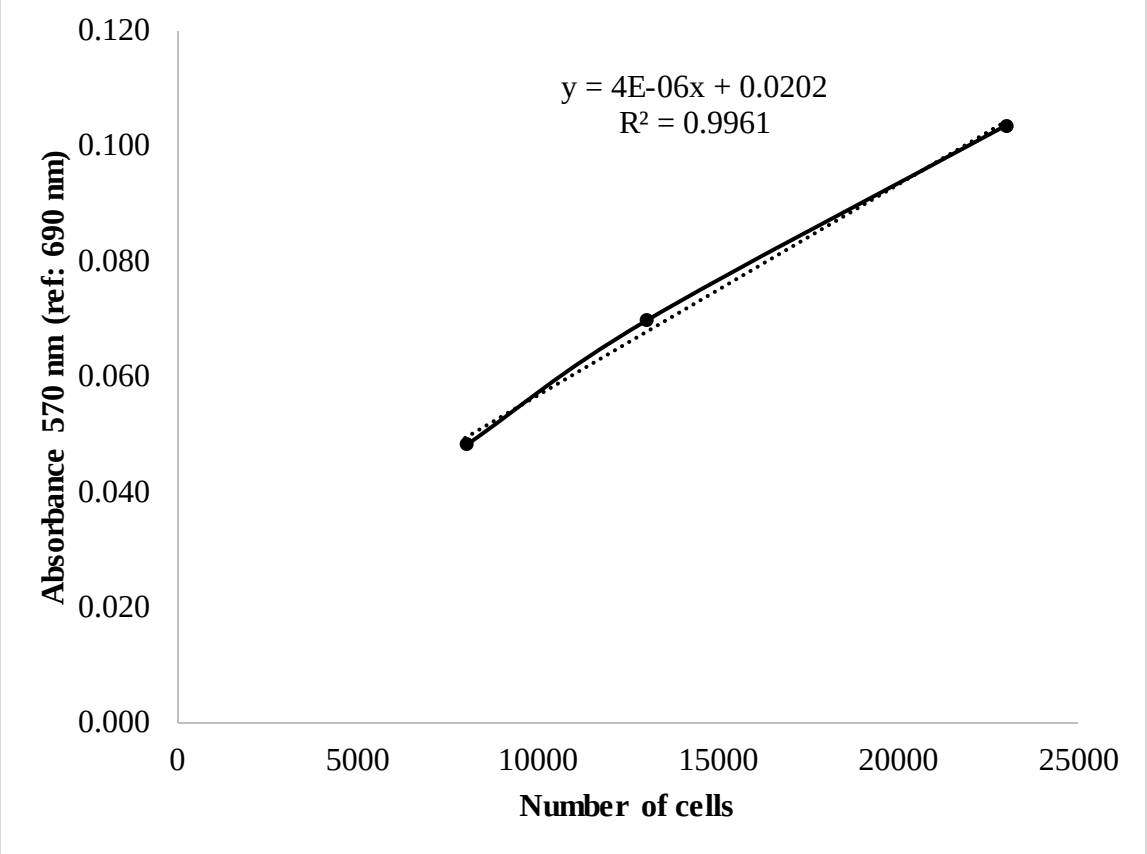

Figure 4.16. The absorbance values of N-HDF cells as a result of MTT analysis depend on the cell number.

4.6.2. Crystal Violet and F-Actin/DAPI Staining

Morphology analysis of n-HDF cells was conducted by crystal violet staining on the 1st, 3rd, and 7th days of the culture and, f-actin/DAPI staining on the 3rd day of culture. It has been observed that n-HDF cells have large nuclei and a very prominent widely spread skeleton. It is also among the observations that n-HDF cells have long filopodia structures and tend to form regular netted structures by contacting each other with the help of these structures. However due to the results of crystal violet staining, in the later days of culture, the cells shrank and formed more spindle structures. Nuclear prominence is reduced. F Actin/ DAPI staining revealed that n-HDF cells have round or oval nuclei and many cytoskeleton filaments (See Figure 4.17 and 4.18).

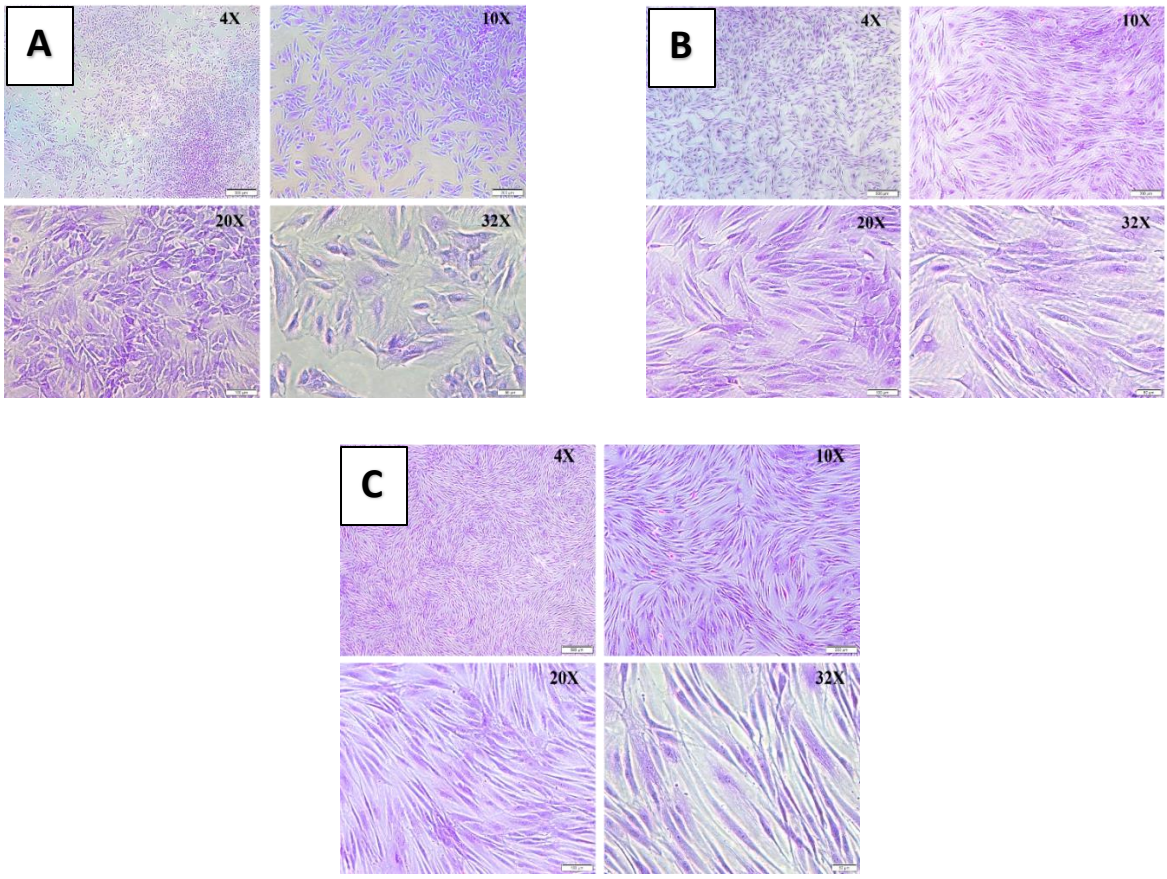

Figure 4.17. Crystal violet staining images of n-HDF cells on the A) 1st, B) 3rd and C) 7th day of culture. With 4X, 10X, 20X and 32X magnifications, respectively.

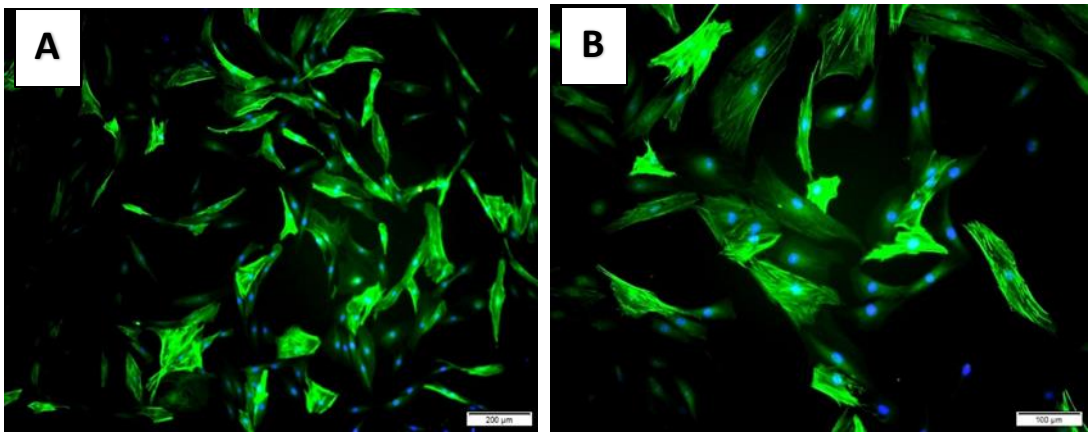

Figure 4.18. F- Actin DAPI staining of the n-HDF cells on 3rd day of culture. A) With 10X B) with 20X magnifications.

4.7. Cell Culture Studies

In tissue engineering (TE) research it is the critical point how biomaterials as matrices and cells interact together [80]. These matrices in the role of extracellular matrix (ECM) for cells must have the ability to create the environment for adhesion, growth, and normal activity of cells to be used in TE and it is noteworthy that mechanical factors affect this interaction [80, 81]. In this research, due to the unknown biocompatibility effect of the fabricated TPS films with different ratios of glycerol and D-sorbitol, cell culture studies were performed. Normal human dermal primary fibroblast cells were selected for culturing on these films and the effect of these TPS films on cell adhesion, growth, and proliferation was investigated. Six selected film groups were examined, however, three groups with 40% (10S-30G), 50% (20S-30G), and 60% (20S-40G) plasticizers showed acceptable results the other three groups did not present promising results.

4.7.1. Determination of Cell Viability

In this research, for determination of the cell viability on TPS films MTT assay and live/dead staining tests were performed on the 1st and 7th days of the culturing.

4.7.1.1. MTT Analysis

MTT assay relies on the mitochondrial capability for the metabolization of the MTT in living cells, by converting the yellow tetrazole salt to purple formazan crystals [82]. The results obtained from the MTT assay of six selected groups of films with 30% (10S-20G), 30% (20S-10G), 40% (10S-30G), 40% (20S-20G), 50% (20S-30G), 60% (20S-40G) plasticizer and n-HDF cells as a control group, which cultured in tissue culture polystyrene dishes (TCPS), showed that in three groups of the films with total plasticizer of 40% (10S-30G), 50% (20S-30G) and 60% (20S-40G) cell viability percentages were higher on the 7th day of the culturing in comparison with other groups.

For this reason, the results of the MTT assay of films with total plasticizers of 60%, 50%, and 40% respectively with D-sorbitol to glycerol ratio of 2/4, 2/3, and 1/3 on the 7th day of culture were examined more precisely with the results of the first day (See Figure 4.19). Statistically, a p value of < 0.05 was accepted as significant. Results from the graph of the cell viability percentage obtained from the MTT assay presented that TCPS as the control group in comparison with cultured films with total plasticizers of 40%, 50%, and 60% respectively, showed significantly higher cell viability percentages in the first day (• $p<$ 0.05). Examination of cell viability results on the seventh day showed that TCPS as the

control group compared to films with 60% plasticizer, had significant higher viability (▪ $p<$ 0.05), and in comparison of the TCPS with groups of films with 40% and 50% plasticizer, respectively, cell viability was extremely significantly higher (▪ ▪ ▪ ▪ $p<$ 0.0001). Results of the seventh day indicated that the group of the film with 60% total plasticizer in comparison with other film groups presented a higher cell viability percentage. A comparison of the results of the 7th and 1st day of the MTT assay revealed that on the 7th day of culture, respectively, the TCPS group and cultured film with 60% plasticizer presented the highly statistically significant proliferation and cell viability, in comparison with the first day's results (** $p<$ 0.01). However, contrary to other cellular test results, which will be discussed, respectively, the films of the groups with 40% and 50% total plasticizer on the seventh day showed a significantly lower percentage of cell viability compared to the first day (* $p<$ 0.05). According to the results of the MTT assay, it can be concluded that increasing the total amount of plasticizers by 60% with a D-sorbitol to glycerol ratio of 2/4 in films, has increased the proliferation and cell viability compared to other samples (See Figure 4.19).

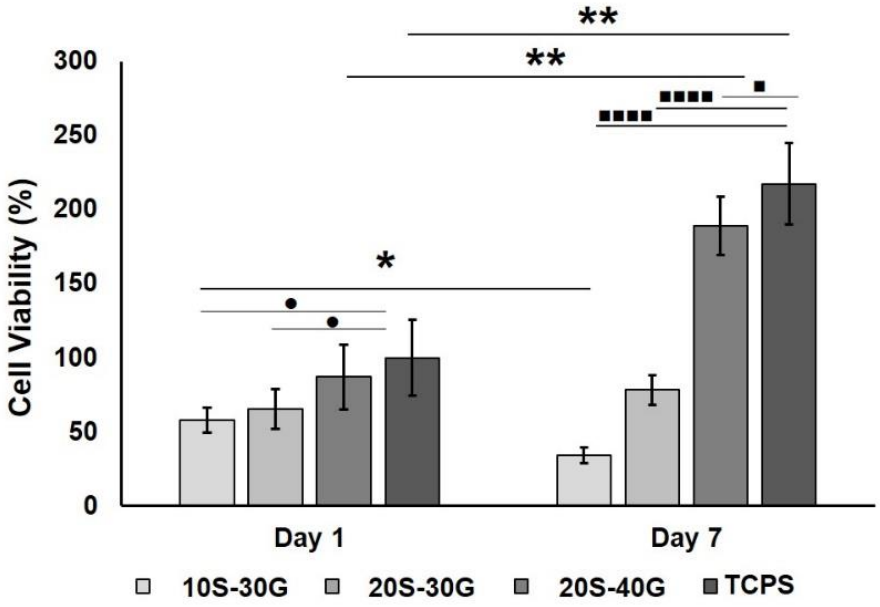

Figure 4.19. MTT results of n-HDF cells cultured on the three selected TPS films with total plasticizer of 40% (10S-30G), 50% (20S-30G), and 60% (20S-40G) (statistically significant differences n = 3, • $p<$ 0.05 when 1st day TCPS is a control group; * $p<$ 0.05, ** $p<$ 0.01 when groups compared within themselves; ▪ ▪ ▪ ▪ $p<$ 0.0001, ▪ $p<$ 0.05 when 7th day TCPS is a control group.

4.7.1.2. Live/Dead Staining

The results obtained from images of the live/dead staining in 1st and 7th days indicated that on the first day of the culture, in all the samples the live cells (green labeled) appeared almost in agglomeration form in different parts of the films and the red points, which indicate dead cells, unlike the living cells, were rarely seen (See Figure 4.20). An image of the live/dead staining of the films with 30% (20S-10G) plasticizer was not obtained.

But on the 7th day of culture, like the MTT assay obtained results, only three groups of the films with total plasticizer of 40% (10S-30G), 50% (20S-30G), and 60% (20S-40G) showed acceptable results. In other groups, either cell agglomeration occurred or no cell staining image was obtained. In the staining of cultured cells on films with a total plasticizer of 40% (10S-30G), 50% (20S-30G), and 60% (20S-40G) on the 7th day, the number of the living cells was much higher than the first day and they have good confluency and spread on the films. The number of dead cells was much less than the number of living cells and more than the number of dead cells on the first day in all samples. Generally, it can be conducted that all the films create suitable matrices for cells to proliferate and have biocompatibility properties. In samples, with total plasticizer of 40% (10S-30G), 50% (20S-30G), and 60% (20S-40G) on the 7th day cells presented a spindle like shape which is the morphology of the typical fibroblast cells [83].

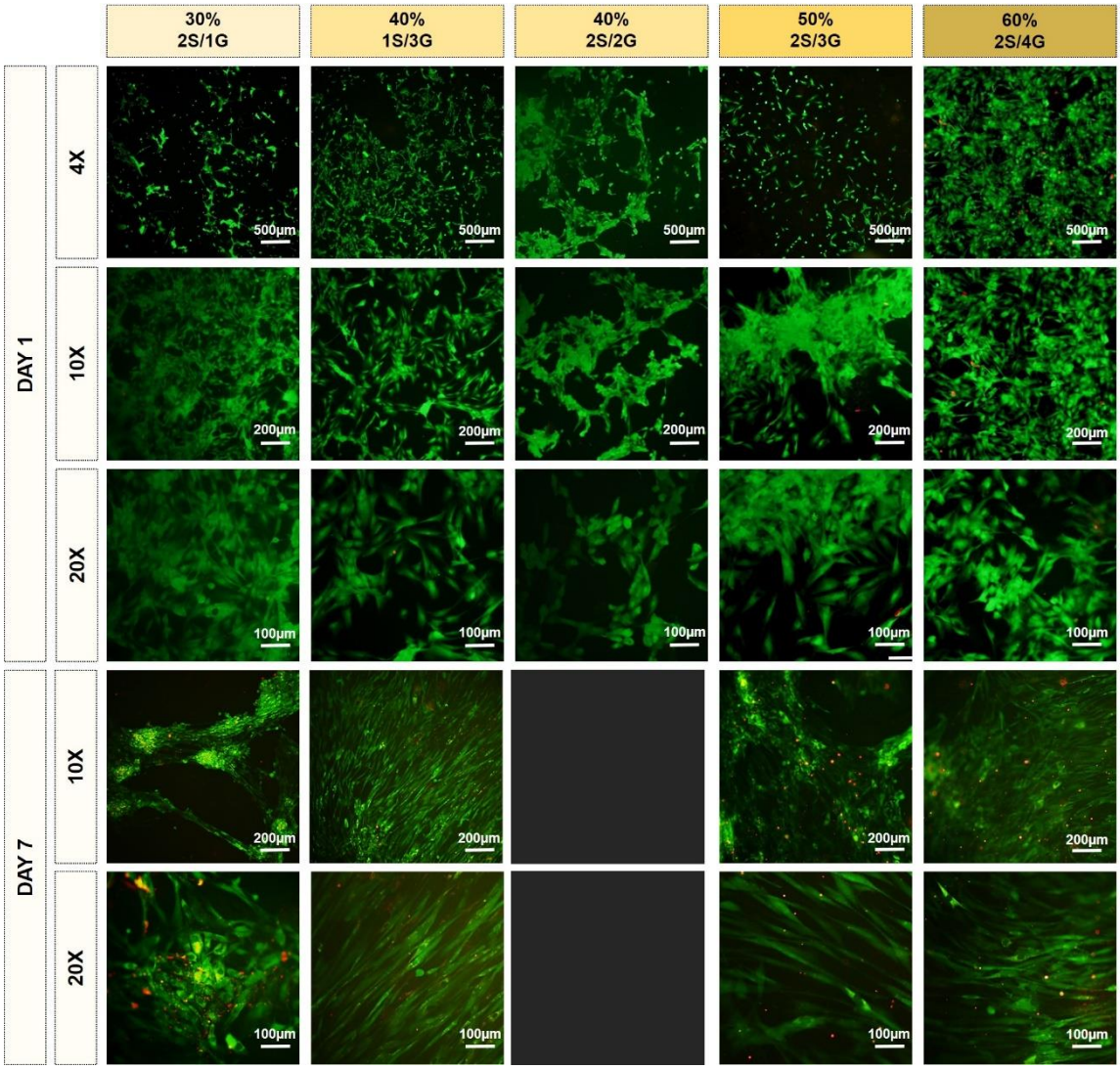

Figure 4.20. Live/Dead staining fluorescence images of the cultured n-HDF cells on the fifth TPS films with total plasticizer of 30% (20S-10G), 40% (10S-30G), 40% (20S-20G), 50% (20S-30G), 60% (20S-40G) in the first and seventh day of culturing at 250X and 500X magnifications. (Green and red markers in live/dead staining indicates live and dead cells, respectively).

4.7.2. Morphology of the cells (SEM Analysis)

The surface of a biocompatible biomaterial should provide a suitable substrate for proliferation, adhesion, and cell migration [84]. SEM analyze conducted to investigate, the morphology and adhesion of the n-HDF cells on the selected TPS films with 30% (10S-20G), 30% (20S-10G), 40% (10S-30G), 40% (20S-20G), 50% (20S-30G), 60% (20S-40G) plasticizer on the 1st and 7th day of culture and to further research about the biocompatibility property of the TPS films. On the first day, cell adhesion was seen in all the films, except in films with 30% (20S-10S) and 40% (10S-30G) plasticizer. On the 7th day of culture

according to the SEM micrographs in all groups of films cell attachment and proliferation has been seen (See Figure 4.21).

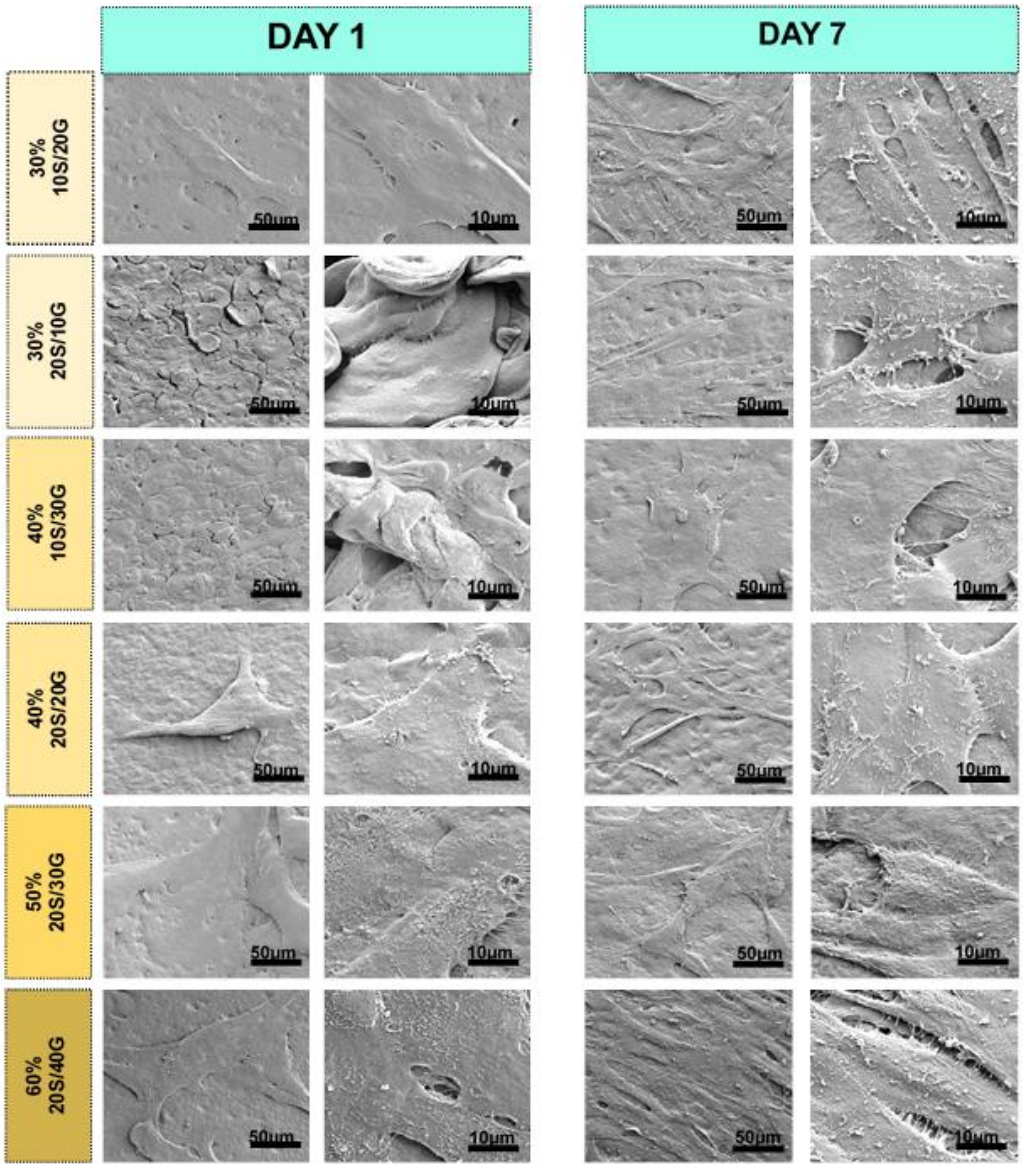

Figure 4.21. SEM images of n-HDF cells in the first and seventh days of culturing on the six selected TPS films with total plasticizer of 30% (10S-20G), 30% (20S-10G), 40% (10S- 30G), 40% (20S-20G), 50% (20S-30G), 60% (20S-40G) at 1000X and 5000X magnification.

According to SEM micrographs, more cell adhesion can be seen in films containing total plasticizers of 40% (10S-30G), 50% (20S-30G), and 60% (20S-40G) respectively. As mentioned above, these films have hydrophilic properties and can promote cell adhesion, and the group with 60% (20S-40G) total plasticizer, which has more hydrophilicity properties than the other three groups, has been a pioneer in this regard. According to the

SEM micrographs, the cells due to the cytoplasm expansion spread on the surface of the films by multiple filopodia. In two groups of these films with 50% (20S-30G) and 60% (20S-40G) total plasticizers, the D-sorbitol ratio is equal but the glycerol increment leads to increasing the total plasticizer ratio of the films which caused to the promotion of the cell's attachment and proliferation and forming of the cells layer on their surfaces (See Figure 4.21).

4.7.3. Cytoskeleton/Nucleus Staining

F-actin/ DAPI staining of the n-HDF cells was performed on the seventh day of the culturing and fluorescent images of the staining presented the F-actin cytoskeleton network in green color and nuclei in blue color. The visible extensive actin filaments networks of the cells and their morphology presented that the cells were well-spread on the surface of TPS films with 40% (10S-30G), 50% (20S-30G), and 60% (20S-40G) plasticizer had good adhesion. In all the samples, on the 7th day of the culture, DAPI staining revealed that cells had an oval or round blue nucleus in the center which presented the nucleus morphology of the typical fibroblast cells [42]. Due to the results obtained from staining, TPS samples with 40% (10S-30G), 50% (20S-30G), and 60% (20S-40G), plasticizer presented well biocompatibility properties and created proper matrices for cell adhesion, proliferation, and spread. However, in other groups, the cells did not have good proliferation (See Figure 4.22 and 4.23).

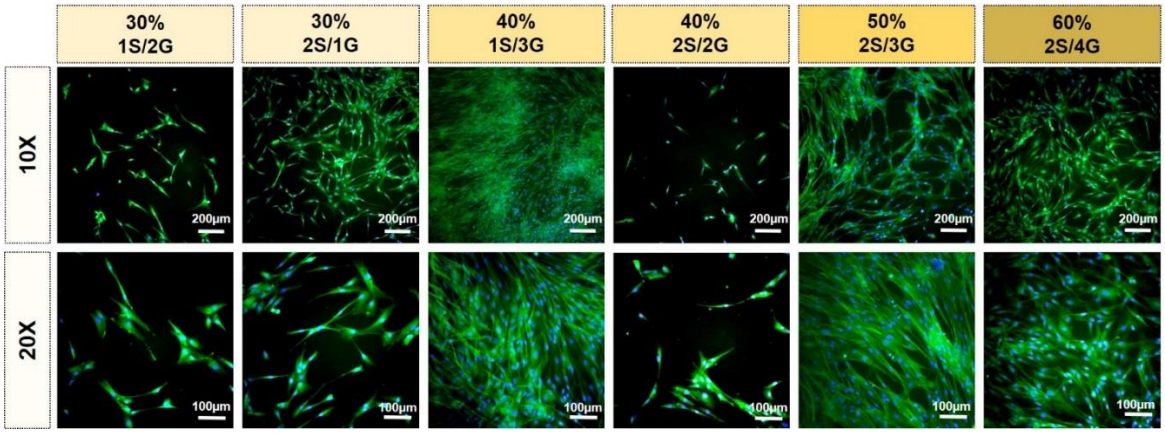

Figure 4.22. Cytoskeleton/nucleus staining fluorescence images of the cultured n-HDF cells on the six selected TPS films with total plasticizer of 30% (10S-20G), 30% (20S-10G), 40% (10S-30G), 40% (20S-20G), 50% (20S-30G), 60% (20S-40G) in the seventh day of culture at 250X and 500X magnifications. (Green and blue fluorescence indicates cell skeleton and cell nucleus, respectively)

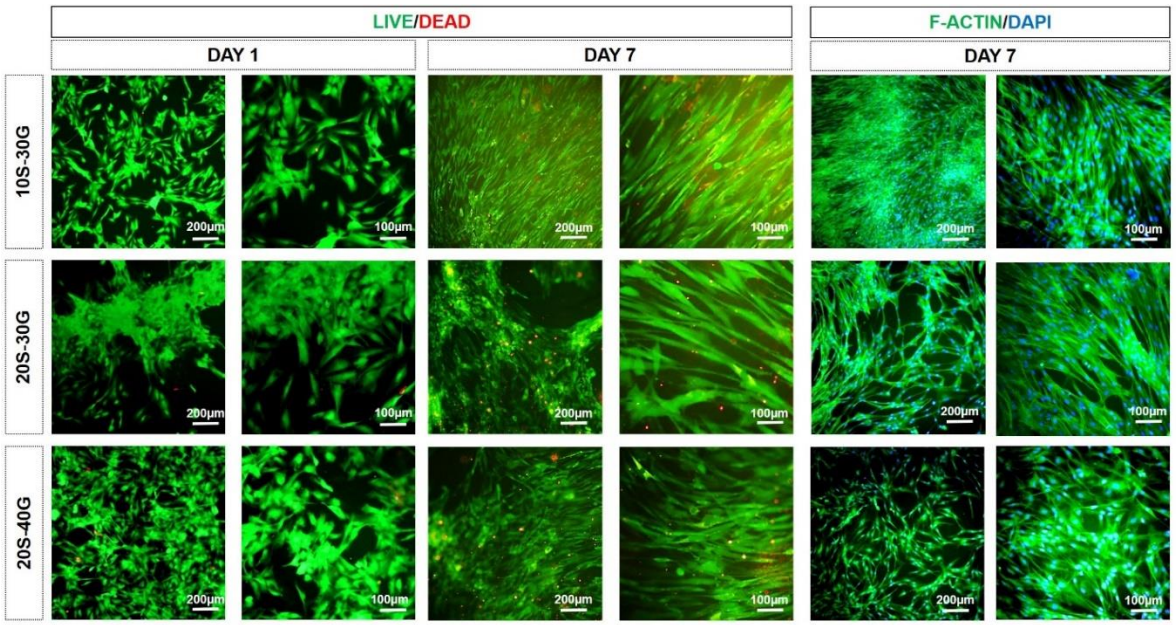

Figure 4.23. Live/Dead and Cytoskeleton/nucleus staining fluorescence images of the cultured n-HDF cells on the three selected TPS films with total plasticizer of 40% (10S- 30G), 50% (20S-30G), and 60% (20S-40G) in the first and seventh day at 250X and 500X magnifications. (Green and red markers in live/dead staining indicates live and dead cells, respectively and in cytoskeleton/nucleus staining Green and blue fluorescence indicates cell skeleton and cell nucleus, respectively)

5. RESULTS AND DISCUSSION

In this part of the thesis, the results obtained from the experiments are discussed in detail and it is presented as a summary and results section. Wheat starch granules have a lenticular shape with indentations and consist of small and large size types [11]. The size of small and large raw wheat starch granules was measured as 19.43 ± 2.80 µm and 5.27 ± 2.37 µm respectively. During the hydration of starch by the water as the most common plasticizer, swelling of granules occurs. If the event simultaneously happened by heating starch to about 60-80°C (depending on the source of starch), irreversible swelling and melting of the crystalline region in granules were occurs [12]. Numerous hydrogen bonds amongst starch macromolecules make starch decompose, before reaching the melting point, under rising temperature conditions. This property can limit the usage of starch in different situations of research, however by modifying starch to thermoplastic starch, the mentioned problem is nearly solvable [12, 13]. In this study, Thermoplastic wheat starch (TPS) films were fabricated with 30% to 70% total plasticizer and different ratios of glycerol and D-sorbitol to evaluate it as a biocompatible biomaterial for application in biomedical and tissue engineering research. The solution casting method is used for this research laboratory experiments in fabricating TPS films to study their mechanical and thermal properties of them. To fabricate TPS films materials such as starch and plasticizers (Water, D-sorbitol, and glycerol) are selected. The plasticizers portion of the films was altered from 30% to 70% depending on the starch weight (3 g) and different ratios of D-sorbitol and glycerol were used in each percentage. It is notable that, in this study, an increase and reduction in the amount of glycerol compared to D-sorbitol in TPS films with the same total plasticizers ratio, respectively had led to an increment in stickiness and brittleness in their appearance. The results obtained from the measurement of the density values revealed that in groups with the same total plasticizer, the density of the films increases by an increment of the D-sorbitol content compared to the glycerol, which is in agreement with other research [55, 56]. It is noteworthy that D-sorbitol and glycerol used in this study have a density of 1.49 g/cm^3 and 1.26 g/cm^3, respectively. The moisture content values of the TPS films indicated that in the groups with the same total plasticizer by reduction of the glycerol ratio to the D-sorbitol, the

moisture contents of the films were reduced. Due to the high molecular similarity of sorbitol with glucose units of the starch polymer, it is likely to establish a strong intermolecular bond in comparison with glycerol and starch chains [55, 57]. In the continuation of the research, the best ten groups of films with total plasticizer: 30% (10S-20G), 30% (20S-10G), 40% (10S-30G), 40% (20S-20G), 50% (10S-40G), 50% (20S-30G), 60% (10S-50G), 60% (20S-40G), 60% (40S-20G), 70% (40S-30G) were selected. About the mechanical properties of films, it should be mentioned that many studies have shown that increases in the plasticizer ratio led to a reduction in the tensile strength values [60, 61]. Tensile strength and elastic modulus measurement indicated that the TPS films with total plasticizer ratios of 30% and 40% had a better performance in comparison with the other ten groups. Six TPS films with total plasticizer ratio of 30% (10S-20G), 30% (20S-10G), 40% (10S-30G), 40% (20S-20G), 50% (20S-30G), 60% (20S-40G) were selected for the next analysis due to their pioneer properties. FTIR results of the raw and dried starch, D-sorbitol, glycerol, and 6 selected groups of the TPS films presented an agreement with other research [55, 63-58]. The obtained results from the hydrolytic degradation test revealed that in the groups of the films with equal total plasticizer, increasing the D-sorbitol to the glycerol ratio, mass loss of the TPS films decreased, which presented lower hydrolytic degradation. This may be due to the fact that D-sorbitol binds more strongly to starch in comparison with glycerol, which increases the water-resistance property of the TPSs, and it is notable, glycerol has more affinity with water [55, 57].

In the determination of water uptake capacities, results indicated that in groups with equal total plasticizers, by increasing the amount of D-sorbitol to glycerol, the water absorption and swelling rate of the films were reduced. The results obtained from tests revealed that an increase in the total amount of the plasticizers led to a decrease in water absorption and swelling of the TPS films other studies also support these results [55, 68]. XRD analysis patterns were presented that the films have less crystallinity than the starch, which is due to the reaction of the plasticizers with the starch chains that leads to the destruction of the starch crystalline network [69]. Also, WCA measurements revealed that starch thermoplastic films have hydrophilic properties [70]. From the results of this test, the group with 60% total plasticizer had the highest hydrophilicity, which is probably due to the high glycerol content, which is more hydrophilic than sorbitol. Additionally, from TGA results, in the groups with the same total plasticizer ratio, increasing the amount of D-sorbitol compared to glycerol

caused more temperature stability in the TPS films. This can be due to lower volatility and a strong bond of the sorbitol with starch in comparison with glycerol [54].

In the endothermic diagram of the DSC of the native wheat starch, three peaks were observed, the first peak was related to the gelatinization temperature of the starch, the second peak was related to the melting temperature of amylose and fat complex and third one was indicated decomposition temperature of the starch which are about 63.9°C, 112.3°C and 270.9°C for raw starch, respectively [76-7]. The data obtained from the DSC results show that TPS films have higher decomposition temperatures due to the presence of plasticizers and an increment in the amount of plasticizer increases the decomposition temperature of the films. SEM analysis of the TPS films' surfaces revealed that increasing the ratio of the glycerol to the D-sorbitol leads to more defects and roughness in the film's surface, which is more visible in higher concentrations of total plasticizer. Roughness analysis of the film surfaces was performed using a perthometer, the results obtained from the tests prove that in groups with the same total plasticizer increasing the D-sorbitol ratio causes a decrease in roughness. Generally, the results obtained from the measurement of roughness support the results obtained from SEM analysis.

For cell culture studies normal human dermal primary fibroblast cells were selected for culturing on these films and the effect of these TPS films on cell adhesion, growth, and proliferation was investigated. Six selected film groups were examined, however, three groups with 40% (10S-30G), 50% (20S-30G), and 60% (20S-40G) plasticizers showed acceptable results the other three groups did not present promising results. Characterization of n-HDF primary cells shows that they have a doubling time of 46.2 h and have large nuclei and a very prominent widely spread skeleton. According to the SEM micrographs, the cells due to the cytoplasm expansion spread on the surface of the films by multiple filopodia. According to SEM micrographs, more cell adhesion can be seen in films containing total plasticizers of 40% (10S-30G), 50% (20S-30G), and 60% (20S-40G) respectively. In two groups of these films with 50% (20S-30G) and 60% (20S-40G) total plasticizers, the D-sorbitol ratio is equal but the glycerol increment leads to increasing the total plasticizer ratio of the films, which caused the promotion of the cell's attachment, proliferation, and forming of the cells layer on their surfaces. Due to the results obtained from F-Actin/ DAPI staining, TPS samples with 40% (10S-30G), 50% (20S-30G), and 60% (20S-40G) plasticizers presented well biocompatibility properties and created proper matrices for cell adhesion, proliferation, and spread, where cells presented a spindle like shape that is the morphology

of the typical fibroblast cells [42]. However, in other groups, the cells did not have good proliferation. MTT assay was performed for the cytotoxicity effect of six selected groups however just TPS groups with 40% (10S-30G), 50% (20S-30G), and 60% (20S-40G) plasticizer presented acceptable results.

Generally, TPS Films with total plasticizers of 30% and 40% presented higher tensile strength, toughness, and elastic modulus values in comparison to films with a total plasticizer of 50%, 60%, and 70%. Increment in the ratio of the D-sorbitol to glycerol in TPS films with equal total plasticizers had led to higher density value and thermal stability, however, reduces moisture absorption, and hydrolytic degradation ratio of the TPS films. Three groups of the films with 60% (20S-40G), 50% (20S-30G), and 40% (10S-30G) respectively, due to the normal human dermal fibroblast cells viability analysis presented higher biocompatibility and proper surfaces for cells adhesion and proliferation. The TPS films showed better mechanical and physical properties at lower percentages, on the contrary, in cell studies, an increment in the percentages of plasticizers led to higher cell adhesion and viability, therefore increasing the biocompatibility of the TPS films.

6. REFERENCES

[1] S. Kumari, R.P. Singh, N.N. Chavan, P.K. Annamalai, Bioinspired, Biomimetic and Nanobiomaterials 7 (**2018**) 219–227.

[2] T. Biswal, Materials Today: Proceedings 41 (**2021**) 397–402.

[3] T. Jiang, Q. Duan, J. Zhu, H. Liu, L. Yu, Advanced Industrial and Engineering Polymer Research 3 (**2019**) 8-18.

[4] M.A.V.T. Garcia, C.F. Garcia, A.A.G. Faraco, Starch - Stärke 72 (**2020**) 190–270.

[5] R.L Whistler, J.N. Bemiller, Starch: Chemistry and Technology (Food Science and Technology), Academic Press, (**2009**)1-879.

[6] A. Blennow, A.M. Bay-Smidt, P. Leonhardt, O. Bandsholm, M.H. Madsen, Starch - Stärke 55 (**2003**) 381–389.

[7] E. Basiak, A. Lenart, F. Debeaufort, International Journal of Biological Macromolecules 98 (**2017**) 348–356.

[8] R.F. Tester, J. Karkalas, X. Qi, Journal of Cereal Science 39 (**2004**) 151–165.

[9] D. Perin, E. Murano, Natural Product Communications 12 (**2017**) 837– 853.

[10] B.M.J. Martens, W.J.J. Gerrits, E.M.A.M. Bruininx, H.A. Schols, Journal of Animal Science and Biotechnology 9 (**2018**) 1-13.

[11] D. Domene-López, J.C. García-Quesada, I. Martin-Gullon, M.G. Montalbán, Polymers 11 (**2019**) 288-295.

[12] W. Cheng, Carbohydrate Polymers 211 (**2019**) 204–208.

[13] F. Kahvand, M. Fasihi, International Journal of Biological Macromolecules 140 (**2019**) 775–781.

[14] H. Li, M.A. Huneault, Journal of Applied Polymer Science 119 (**2010**) 2439–2448.

[15] E. Troy, M.A. Tilbury, A.M. Power, J.G. Wall, Polymers 13 (**2021**) 3321.

[16] J. Courtenay, R. Sharma, J. Scott, Molecules 23 (**2018**) 654.

[17] R.J. Hickey, A.E. Pelling, Frontiers in Bioengineering and Biotechnology 7 (**2019**) 45.

[18] N. Lin, A. Dufresne, European Polymer Journal 59 (**2014**) 302–325.

[19] D.S. Jackson, Encyclopedia of Food Sciences and Nutrition (**2003**) 5561–5567.

[20] I.J. Tetlow, E. Bertoft, International Journal of Molecular Sciences 21 (**2020**) 7011.

[21] N.H. Zakaria, N. Muhammad, M.M.A.B. Abdullah, Materials Science and Engineering 209 (**2017**) 012087.

[22] Y.I. Cornejo-Ramírez, O. Martínez-Cruz, C.L. Del Toro-Sánchez, F.J. Wong-Corral, J. Borboa-Flores, F.J. Cinco-Moroyoqui, CyTA - Journal of Food 16 (**2018**) 1003–1017.

[23] K. Dome, E. Podgorbunskikh, A. Bychkov, O. Lomovsky, Polymers 12 (**2020**) 641.

[24] R.D. Hancock, B.J. Tarbet, Journal of Chemical Education 77 (**2000**) 988.

[25] E. Bertoft, Agronomy 7 (**2017**) 56.

[26] D. Donmez, L. Pinho, B. Patel, P. Desam, O.H. Campanella, Current Opinion in Food Science 39 (**2021**) 103–109.

[27] B.Miller, R. Derby, et al., Cereal Chemistry (**1973**) 271-280.

[28] M. Potts, Journal of Food Composition and Analysis 8 (**1995**) 371.

[29] J.A Delcour, R.C. Hoseney, Principles of Cereal Science and Technology, 3rd edition, Cereals & Grains Associations, AACC International, Inc., (**2010**) 33–45

[30] H. Koksel, A. Basman, Cereal Foods World (**2008**) 317-318.

[31] H. Ibrahim, M. Farag, H. Megahed, S. Mehanny, Carbohydrate Polymers 101 (**2014**) 11–19.

[32] A.P. Mathew, A. Dufresne, Biomacromolecules 3 (**2002**) 609–617.

[33] M.L. Méndez-Hernández, J.L. Rivera-Armenta, Z. Sandoval-Arellano, B.A. Salazar-Cruz, M.Y. Chavez-Cinco, Applications of Modified Starches (**2018**) 1-39.

[34] K. Krogars, J. Heinämäki, M. Karjalainen, A. Niskanen, M. Leskelä, J. Yliruusi, International Journal of Pharmaceutics 251 (**2003**) 205–208.

[35] Y. Habibi, L.A. Lucia, Polysaccharide Building Blocks, John Wiley & Sons, (**2012**) 278-306

[36] K. Koch, T. Gillgren, M. Stading, R. Andersson, International Journal of Biological Macromolecules 46 (**2010**) 13–19.

[37] L. Mościcki, M. Mitrus, A. Wójtowicz, T. Oniszczuk, A. Rejak, L. Janssen, Food Research International 47 (**2012**) 291–299.

[38] Y. Zhang, C. Rempel, Q. Liu, Critical Reviews in Food Science and Nutrition 54 (**2014**) 1353–1370.

[39] H.A. Pushpadass, M.A. Hanna, Industrial & Engineering Chemistry Research 48 (**2009**) 8457–8463.

[40] H.A. Pushpadass, D.B. Marx, M.A. Hanna, Starch - Stärke 60 (**2008**) 527–538.

[41] H.A. Pushpadass, P. Bhandari, M.A. Hanna, Carbohydrate Polymers 82 (**2010**) 1082–1089.

[42] M. Ravikanth, P. Soujanya, K. Manjunath, T. Saraswathi, C. Ramachandran, Journal of Oral and Maxillofacial Pathology:JOMFP 15 (**2011**) 247–250.

[43] I.R. Fernandes, F.B. Russo, G.C. Pignatari, M.M. Evangelinellis, S. Tavolari, A.R. Muotri, P.C.B. Beltrão-Braga, Cytotechnology 68 (**2014**) 223–228.

[44] M.A. Kisiel, A.S. Klar, Skin Tissue Engineering (**2019**) 71–78.

[45] M.A. Asl, S. Karbasi, S. Beigi-Boroujeni, S. Zamanlui Benisi, M. Saeed, International Journal of Biological Macromolecules 191 (**2021**) 500–513.

[46] C. Koski, B. Onuike, A. Bandyopadhyay, S. Bose, Additive Manufacturing 24 (**2018**) 47–59.

[47] E. Naseri, C. Cartmell, M. Saab, R.G. Kerr, A. Ahmadi, Macromolecular Bioscience 21 (**2021**) 2100368.

[48] P.F. Builders, M.I. Arhewoh, Starch - Stärke 68 (**2016**) 864–873.

[49] E. Alp, F. Damkaci, E. Guven, M. Tenniswood, International Journal of Nanomedicine 14 (**2019**) 1335–1346.

[50] N.N. Ab'lah, T.W. Wong, Polymer Science and Innovative Applications (**2020**) 287–330.

[51] F.G. Torres, O.P. Troncoso, C.G. Grande, D.A. Díaz, Materials Science and Engineering: C 31 (**2011**) 1737–1740.

[52] Z. Xie, J. Guan, L. Chen, Z. Jin, Y. Tian, Starch - Stärke 70 (**2018**) 1700218.

[53] R. Yoksan, N. Khanoonkon, C. Yokesahachart, N. Noivoil, K. Dang, International Journal of Materials and Metallurgical Engineering , (**2015**) 1166-1170.

[54] M.L. Sanyang, S.M. Sapuan, M. Jawaid, M.R. Ishak, J. Sahari, Journal of Food Science and Technology 53 (**2015**) 326–336.

[55] S.M.A. Razavi, A. Mohammad Amini, Y. Zahedi, Food Hydrocolloids 43 (**2015**) 290–298.

[56] M.A. Cerqueira, B.W.S. Souza, J.A. Teixeira, A.A. Vicente, Food Hydrocolloids 27 (**2012**) 175–184.

[57] M. Chiumarelli, M.D. Hubinger, Food Hydrocolloids 38 (**2014**) 20–27.

[58] C.M.O. Müller, F. Yamashita, J.B. Laurindo, Carbohydrate Polymers 72 (**2008**) 82–87.

[59] A.B. Dias, C.M.O. Müller, F.D.S. Larotonda, J.B. Laurindo, Journal of Cereal Science 51 (**2010**) 213–219.

[60] M. Ghasemlou, F. Khodaiyan, A. Oromiehie, Carbohydrate Polymers 84 (**2011**) 477–483.

[61] T.J. Gutiérrez, N.J. Morales, E. Pérez, M.S. Tapia, L. Famá, Food Packaging and Shelf Life 3 (**2015**) 1–8.

[62] A. Kurt, T. Kahyaoglu, Carbohydrate Polymers 104 (**2014**) 50–58.

[63] F.M.B. Coutinho, M.C. Delpech, L.S. Alves, Journal of Applied Polymer Science 80 (**2001**) 566–572.

[64] V.P. Indran, N.A. Syuhada Zuhaimi, M.A. Deraman, G.P. Maniam, M.Mohd. Yusoff, T.-Y. Yun Hin, M.H. Ab. Rahim, RSC Adv. 4 (**2014**) 25257–25267.

[65] S. Quinquenet, M. Ollivon, C. Grabielle-Madelmont, M. Serpelloni, Thermochimica Acta 125 (**1988**) 125–140.

[66] S.-N. Yuen, S.-M. Choi, D.L. Phillips, C.-Y. Ma, Food Chemistry 114 (**2009**) 1091–1098.

[67] S. Lyu, D. Untereker, International Journal of Molecular Sciences 10 (**2009**) 4033–4065.

[68] O. Lopez, M.A. Garcia, M.A. Villar, A. Gentili, M.S. Rodriguez, L. Albertengo, LWT - Food Science and Technology 57 (**2014**) 106–115.

[69] N. Leblanc, R. Saiah, E. Beucher, R. Gattin, M. Castandet, J.-M. Saiter, Carbohydrate Polymers 73 (**2008**) 548–557.

[70] M. Pervaiz, P. Oakley, M. Sain, Materials Sciences and Applications 05 (**2014**) 845–856.

[71] Gutiérrez, R. Ollier, V.A. Alvarez, Springer Series on Polymer and Composite Materials (**2017**) 131–158.

[72] S.M. Ojagh, M. Rezaei, S.H. Razavi, S.M.H. Hosseini, Food Chemistry 122 (**2010**) 161–166.

[73] D. Cuvelier, M. Théry, Y.-S. Chu, S. Dufour, J.-P. Thiéry, M. Bornens, P. Nassoy, L. Mahadevan, Current Biology 17 (**2007**) 694–699.

[74] C. Herniou--Julien, J.R. Mendieta, T.J. Gutiérrez, Food Hydrocolloids 89 (**2019**) 67–79.

[75] M.L. Sanyang, S.M. Sapuan, M. Jawaid, M.R. Ishak, J. Sahari, Journal of Food Science and Technology 53 (**2015**) 326–336.

[76] D. Sievert, Y. Pomeranz, A. Abdelrahman, Cereal Chemistry (**1988**) 10-13.

[77] L. Gruchala, Y. Pomeranz, Cereal Chemistry (**1993**) 163-172.

[78] D. Siever, Z. Czuchajowska, Y. Pomeranz, Cereal Chemistry (**1991**).

[79] C.J. Bettinger, R. Langer, J.T. Borenstein, Angewandte Chemie International Edition 48 (**2009**) 5406–5415.

[80] J.A. Sanz-Herrera, E. Reina-Romo, International Journal of Molecular Sciences 12 (**2011**) 8217–8244.

[81] D.E. Discher, Science 310 (**2005**) 1139–1143.

[82] J. van Meerloo, G.J. Kaspers, J. Cloos, Methods in Molecular Biology (**2011**) 237–245.

[83] H. Lu, T. Hoshiba, N. Kawazoe, I. Koda, M. Song, G. Chen, Biomaterials 32 (**2011**) 9658–9666.

[84] J.M.C. Santos, D.R.S. Travassos, P. Ferreira, D.S. Marques, M.H. Gil, S.P. Miguel, M.P. Ribeiro, I.J. Correia, C.M.S.G. Baptista, Journal of Materials Research 33 (**2018**) 1463–1474.